Synthesis of Oxidized Carboxymethyl Cellulose-Chitosan & its Composite Films with SiC and Silica-coated SiC Nanoparticles for Dye Adsorption Study

By

Aiman Javed

Reg. NO. 00000365174

This thesis is submitted as partial fulfillment of requirements for the degree of

MASTER OF SCIENCE IN

CHEMISTRY

Supervised By: Dr. Shahid Ali Khan

Department of Chemistry, School of Natural Sciences,

National University of Sciences and Technology, (NUST),

Islamabad, Pakistan.

2023

THESIS ACCEPTANCE CERTIFICATE

Certified that final copy of MS thesis written by **Aiman Javed** (Registration No. **00000365174**), of **School of Natural Sciences** has been vetted by undersigned, found complete in all respects as per NUST statutes/regulations, is free of plagiarism, errors, and mistakes and is accepted as partial fulfillment for award of MS/M.Phil degree. It is further certified that necessary amendments as pointed out by GEC members and external examiner of the scholar have also been incorporated in the said thesis.

Signature: _____

Name of Supervisor: Dr. Shahid Iqbal

Date: 09/08/2023

Signature (HoD): _____

Date: 10/08/2023

Signature (Dean/Principal): _____

Date: 11/8/2023

National University of Sciences & Technology

MS THESIS WORK

We hereby recommend that the dissertation prepared under our supervision by: Aiman Javed, Regn No. 00000365174 Titled: Synthesis of Oxidized Carboxymethyl Cellulose-Chitosan and Its Composite Films with SiC and Silica-Coated SiC Nanoparticles for Dye Adsorption Study be Accepted in partial fulfillment of the requirements for the award of **MS** degree.

Examination Committee Members

1. Name: PROF. MUDASSIR IQBAL   Signature:_____

2. Name: DR. MUHAMMAD ADIL MANSOOR   Signature:_____

Supervisor's Name DR. SHAHID ALI KHAN   Signature:_____

_____
Head of Department

_____
3/8/23
Date

COUNTERSINGED

_____
Dean/Principal

Date: 03/08/2023

بسم الله الرحمن الرحيم

Dedication

*Dedicated To My Unwavering Pillars of Support, My Beloved Parents, "**Javed Ahmad** and **Abida Parveen**".*

Statement of Original Authorship

I, **Aiman Javed,** hereby state that my MS thesis titled **"Synthesis of Oxidized Carboxymethyl Cellulose-Chitosan & its Composite Films with SiC and Silica-coated SiC Nanoparticles for Dye Adsorption Study"** is my work and has not been submitted previously by me for taking any degree from this National University of Science and Technology or anywhere else in the country/ world.

At any time if my statement is found to be incorrect even after I graduate, the university has the right to withdraw my MS degree.

Name of Student: Aiman Javed

Date: ------------------------------

Signature: ------------------------

ACKNOWLEDGMENTS

Abstract

Environmental pollution due to discharge of synthetic dyes into water bodies has become a critical issue in recent times. To address this challenge, the present study focuses on the development of innovative and eco-friendly adsorbents for efficient dye removal. The aim of this research is to synthesize oxidized carboxymethyl cellulose-chitosan and its composite films, incorporating silicon carbide (SiC) and silica-coated SiC nanoparticles, and evaluate their performance for dye adsorption. The resulting composite films were characterized by using various analytical techniques, including Fourier-transform infrared spectroscopy (FTIR), X-ray diffraction (XRD), Thermogravimetric analysis (TGA), scanning electron microscopy (SEM), and energy-dispersive X-ray spectroscopy (EDX).

The dye adsorption properties of the synthesized composite films were comprehensively investigated. Batch adsorption experiments were conducted using MB dye solution, and the effects of parameters such as contact time, initial dye concentration, catalyst dosages, temperature and pH were systematically evaluated. The adsorption kinetics and isotherms were analyzed to understand the adsorption mechanism and factors influencing the adsorption process. The experimental results demonstrated that pure oxidized carboxymethyl cellulose-chitosan films have high dye adsorption capabilities as compared to its nanocomposite films with SiC and silica-coated SiC nanoparticles. The incorporation of SiC and silica coated SiC nanoparticles blocked the active sites and thereby reduced dye adsorption efficiency. The synthesized oxidized carboxymethyl cellulose-chitosan composite films with SiC and silica-coated SiC nanoparticles present a promising and environmentally friendly approach to mitigate dye pollution from aqueous systems.

Table of Contents

LIST OF FIGURES AND TABLES

LIST OF ABBREVIATIONS

FTIR	Fourier transform infrared spectroscopy
SEM	Scanning electron microscopy
TGA	Thermogravimetric analysis
EDX	Energy-despersive X-ray spectroscopy
XRD	X-ray Diffraction
CMC	Carboxymethyl Cellulose
OCMC	Oxidized Carboxymethyl Cellulose
CS	Chitosan
MB	Methylene Blue
MO	Methyl Organge
CV	Crystal Violet
PVA	Polyvinyl Alcohal

CHAPTER 1

1. **INTRODUCTION**

1.1.   **Background**

Water pollution has emerged as a critical global issue, requiring conservation, security, and management of this important natural resource. Wastewater treatment is necessary to make it suitable for drinking and household purposes using low-cost and efficient techniques. Pollutants like heavy metals and dyes can have toxic and carcinogenic effects, and the textile industry is a leading contributor to water pollution. Heavy metals and dyes are non-biodegradable, accumulate in the body, and cause harmful effects in living organisms. Nanotechnology has gained immense attention in recent years for wastewater treatment, with various nanocomposites being used to remove pollutants from wastewater sources more efficiently than conventional methods. [1]

1.1.1. **Textile effluents**

The textile industry uses a lot of water, much of which is discharged into the environment as effluent. Fig. 1.1 displays the percentage of wastewater from various companies that contains dyes and is released into nearby rivers. The primary cause of pollution is the textile industry's effluent, which contains substantial amounts of a variety of colors. Ten to twenty-five percent of the textile dye is lost during the dying process, and an additional eleven to sixteen percent of the dye ends up in the wastewater.
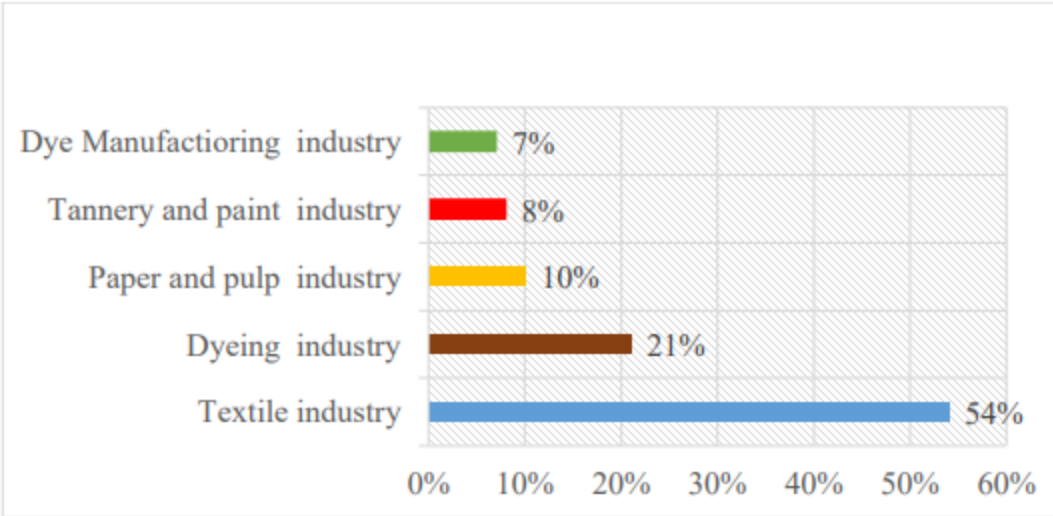
Figure 1.1 Contribution of different industries to discharge of dye-containing wastewater

1.2. Dye Adsorption

Adsorption has proven to be a viable approach due to its advantages of ease of manufacture, operability, efficiency, and low relative cost [2]. The form and chemistry of adsorbents influence their efficacy in adsorption processes [3]. Composite adsorbents can be made in a variety of shapes, including beads, flakes, powders, sheets, and films [4]. Although dispersed adsorbents such as beads, flakes, and powders have a high active surface area, they are difficult to separate from the final product following process treatment. Film-based adsorbents are chosen over other types of adsorbents because they are easier to separate after the procedure and do not require post-treatment filtration. Other benefits of film type adsorbents include increased adsorption capacity, faster kinetics, improved reusability, ease of stacking and scale-up, and the possibility of non-adsorptive separation mechanisms that improve filtration performance. As a result, film-based adsorbents have grown in popularity for removing dangerous compounds from water resources, such as dyes and heavy metal ions [3]. These materials are often present in trace amounts, and film adsorbents

offer an effective and attractive solution for their removal. Metal nanoparticles, metal sulfides, metal oxides, fullerenes, graphite, carbon nanotubes, and other nanoparticles are used in nanocomposites have excellent adsorption capacity due to their higher surface area, making them suitable for water purification. There are several methods for removing color from wastewater, including film separation, aerobic and anaerobic degradation using different microbes, chemical oxidation, coagulation, and flocculation, and adsorption utilizing various adsorbents [4]. Adsorption is now a cost-effective and efficient method for removing pollutants such as dyes and heavy metal ions from water bodies, resulting in their purification [5].

Dye adsorption is the process by which dyes are removed from a solution and adhere to the surface of a solid material, such as activated carbon, zeolites, or other types of adsorbents. This method is widely used in the treatment of wastewater, notably for removing colored pollutants from industrial effluents. The adsorption of dyes onto solid surfaces is a result of various interactions, such as electrostatic forces, hydrogen bonding and van der Waals forces. The efficiency of dye adsorption is influenced by factors such as pH, temperature, contact time, and the initial concentration of the dye in the solution. The extent of dye removal can be determined by measuring the concentration of dye in the solution before and after the adsorption process, and the process can be optimized by adjusting the conditions to achieve maximum adsorption capacity [6].

1.3.   Importance of Films and their nanocomposites

Films are transparent, specialized materials that divide two distinct areas or phases, enabling some things to pass through while blocking or rejecting others. Membranes are thin barriers or selective materials **[7].** After a long time of being prompted by biological membranes and doubts about the

eventual technological viability, film technologies are now being industrially produced on an astonishingly large scale **[8].** Depending on the individual application and desired separation features, they can be synthesized by various materials, including polymers, ceramics, metals, and composites. Based on their structure, material composition, and separation methods, membranes can be categorized **[7].** The traditional method of creating membranes involves pouring a solution of polymer over the proper surface and letting the resulting film set. The dimensions of the membrane's pores determine the permeability of the substrate. These can then be modified by altering the solutions', polymer(s), and casting conditions' compositions **[9].** Film separation efficiency is proportional to permeability and, thus, membrane thickness. The more porous the membrane, the thinner it is **[10].** Polymers are large molecules that are formed of monomers, which are repeating units. They are made up of lengthy, chemically connected chains or networks of monomer units. These monomers may be identical or dissimilar, resulting in a vast range of polymers with various structures and characteristics. Polymeric membranes have a wide range of applications, including fuel cells, medical devices, industrial processes, water treatment, and gas separation. The ability to remove toxins and pollutants from water sources is made possible by membrane technology, which is crucial in the treatment of wastewater. **[11]**

Composites are made up of two or more basic materials with significantly differing chemical, physical, and mechanical properties. The specific characteristics of these composites are due to the unique attributes of the components that comprise them, and also to their relative proportions of volume and compositions within the material system. Depending on the intended use, composites can be designed to meet specific geometrical, structural, chemical, biological, and even aesthetic requirements. These synthetic materials are utilized in a range of industries, including constructions (buildings and dams), the automotive industry (car bodywork), aviation, the military

(ships and boats), and biomedicine. Regardless of considering that metal-based, polymeric, and ceramic composites have been employed in the biomedical profession for decades, composites have recently become popular in medicine. Composites fulfil the desired functions without putting their proximal surrounding tissues or the overall body system at risk, either by promoting tissue repair/healing or by totally replacing the tissue. So, unlike metallic, polymeric, and ceramic biomaterials, composite materials have design flexibility and are simple to adapt to have practically any desired property combinations by the simplest manipulations of different parameters such as the constituents' volume ratios, fiber particle size, geometry, orientation and distribution, matrix type, and so on [12].

1.4.   Why chemically modified carboxymethyl cellulose?

Cellulose is a linear polysaccharide and made up of D-glucopyranose rings through β (1–4) glycosidic bond. As a natural organic polymer compound, it has many distinctive features such as its biodegradability, non-toxicity and compatibility. Because of these features, cellulose has wide applications in industries. Natural cellulose has poor solubility and high crystallinity. Because of these characteristics, the use of cellulose in industries is restricted so human society needs to improve the functionality of cellulose by breaking bonds of molecular chain of cellulose and introducing new groups either by physical, chemical or biological approaches which decreases the crystallinity of cellulose. In such manner, cellulose can be changed into different derivatives that have improved functionality and many applications in different fields.

Carboxymethyl cellulose (CMC) is a kind of anionic water-soluble derivative of cellulose. As a natural polysaccharide, CMC is one of the finest renewable sources for human society. CMC, a

type of water-soluble cellulose ether that differs from natural cellulose materializes in the form of sodium salt that is produced as a result of reaction of alkali cellulose with sodium monochloroacetate under controlled conditions. Functionality of CMC can be increased by modification of CMC through oxidation. In this way, the hydroxyl group of CMC converts into dialdehyde by the cleavage of $C_2\_\_C_3$ bond of glucose unit. There are many other ways of modification of CMC as we use traditional oxidation method to introduce carboxylic group by using inorganic oxidants such as N_2O_4 and NaOCl.

CMC has numerous applications in the field of medicine such as formation of gels through CMC that have major role in thoracic, heart and cornea surgery and it is also used in wound dressing because of its high antimicrobial activity. In thorax surgery, lungs are affixed and then masked by CMC solution so that there's no air leakage and to prevent fluid entrance. The CMC solution can also be injected into the joints of the bones like wrists, hips and knee joints to protect them from swelling and possible demolition of cartilage attached to the bones. CMC is not soluble in the stomach because of the acidic nature of stomach and soluble in basic media of intestine. In the medical field, CMC is used as a coating material for tablets with low viscosity and high degree of purity. It is also used in drug delivery. CMC is also frequently used in the pharmaceutical, cosmetic, and food industries to enhance the consistency, flow, and stability of edible films. CMC has grown into the product preference in the textile industry, as well as in epoxy dispersion paints, adhesives and printing pigments, and coating colors for the paper and pulp industries, due to its favorable price-to-performance ratio. [13].

In order to further enhance the activity of oxidized CMC, it was cross-linked with chitosan to form OCMC-Chitosan network Chitosan (CS), the derivative of chitin, is the second most prevalent

biopolymer after cellulose and comes from a natural, renewable source. Its chemical structure is comparable to that of cellulose. It is a polymer made by deacetylating chitin that contains cationic groups [13]. It is a versatile and environmentally acceptable antifouling substance that has β-(1,4)-2-acetamino-2-deoxy-D-glucose binary linear units. Chitosan's stiff crystalline form causes it to have a poor solubility in water, which prevents it from being used effectively in a variety of operations. Chitosan has demonstrated extraordinary qualities including affordability, accessibility, biocompatibility, biodegradability, nontoxicity, antibacterial activity, low immunogenicity, and nontoxicity. In medicine and biotechnology, natural polymers like chitosan are receiving a lot of interest [14].

CMC has various advantages over chitosan hydrogels, including enhanced moisture absorption, greater water dissolution, biocompatibility, biodegradability, antioxidant activity, antibacterial characteristics, and a higher capacity for metal ion sorption. These advantages are due to CMC's greater number of binding groups and improved chain flexibility [15].

Chitosan is a naturally occurring polymer that has recently gained popularity due to its great capacity for organic color adsorption. This is because active sites, such as hydroxyl and amino groups, can interact with diverse organic and inorganic moieties via physical and chemical forces [16]. In acidic conditions, the amino groups in chitosan can significantly adsorb anionic dyes via electrostatic attraction. It is vital to highlight, however, that the pH threshold for chitosan should be considered in real applications [17]. Chitosan's adsorptive characteristics are mostly attributable to the lone pair electrons of its N and O atoms. Chitosan can be positively charged in the presence of enough protons, or a negative charge in sufficient quantities of basic media [1].

Chitosan has been used for extraction and adsorption in water decontamination, offering a low-cost and sustainable technique for environmental protection [16].

1.5.   Why OCMC-CS silicon Nanocomposites?

The application fields of OCMC-CS complex can be expanded. So, for this purpose, OCMC-CS silicon Nanocomposites were prepared. The mechanical properties of OCMS-CS-SiNPs showed superior mechanical properties with respect to OCMC-CS [18].

The semiconducting material silicon carbide (SiC) has displayed extraordinary qualities, including strong strength, high thermal conductivity, and good heat high chemical inertness, moderate thermal expansion, and shock resistance. Because of these unique properties, SiC is an excellent choice for catalyst support at high temperatures and in harsh environments. SiC must have a porous structure and a large specific surface area for this application. The synthesis of porous SiC has been reported using a variety of techniques. The most popular techniques include shape memory synthesis, carbothermal reduction, electrochemical etching of large SiC, and nano casting. Because of the low cost of raw ingredients and simple reaction equipment, carbothermal degradation of silicon oxide is one of the most effective and controllable methods of porosity of SiC synthesis. When making porous SiC via carbothermal reduction, carbonized organic matter is employed as the carbon source instead of mesoporous silica molecular sieve or silica sol made with TEOS. After heating carbon-silica composites between 1250 and 1450 C, porous SiC is produced [19].

The qualities of powder can be improved, or a new function can be added to the powder by surface modification. Core-shell holds promise for changing the composition of powder. Core-shell composites come in a variety of forms, including catalysts made of Au/Pd-Fe2O3, Ge/Si

nanowires, ionic liquid ZnO nanocrystals, semiconductor nanoparticles (CdSe/ZnS), organic core/inorganic shell nanocomposites, and many other useful composites [20].

In this study, to further improve the properties of SiC nanoparticles, modify the surface of SiC by coating SiO_2 on the surface of SiC nanoparticles by sol-gel method. By breaking the cell membrane and producing oxidative stress, silica-coated silicon carbide nanoparticles have been proven to suppress bacterial growth. These nanoparticles have the ability to penetrate the cell wall of bacteria and contact intracellular components, resulting in cell death. Additionally, the silica coating on the silicon carbide nanoparticles may enhance their stability and prevent aggregation, ensuring their efficient interaction with bacterial cells.

Studies have reported the antibacterial activity of silica-coated silicon carbide nanoparticles against a variety of bacterial species, including Gram-positive and Gram-negative bacteria. Silica-coated silicon carbide nanoparticles have shown great potential as a novel antibacterial agent, and further research in this field may lead to the development of new antibacterial therapies. However, more studies are needed to completely comprehend the mechanism of action and potential toxicity of these nanoparticles [21].

1.6.   Role of PVA

A synthetic polymer called polyvinyl alcohol (PVA) is created by the polymerization of vinyl acetate that further undergoes hydrolysis. PVA is a copolymer made up of hydroxyl and acetyl units that were left over after partial hydrolysis of poly (vinyl acetate) [22]. It is soluble in water and widely used as a binder in the synthesis of polymer membranes. PVA can be combined and processed with other polymer elements, such as those with selective separation capabilities, with

ease. Due to its superior film-forming abilities, PVA can be cast or coated onto a substrate to create a thin, uniform membrane. This skill is essential for producing membranes that are thin, flawless, and of controllable thickness [23].

The different components of a membrane can be joined together by PVA since it has strong adhesive and cohesion qualities [24]. PVA has a strong capability to blend with other polymers to improve or change particular membrane qualities like permeability, selectivity, and mechanical strength. PVA is regarded as environmentally safe, non-toxic [25].

These characteristics make it appropriate for use as water filtration membranes, medication delivery systems, and biomedical devices [26].

PVA may potentially create a crosslinked network with the two polysaccharides when it is introduced to a mixture of oxidized carboxymethyl cellulose (CMC) and chitosan by a variety of methods, including physical entanglements, hydrogen bonds, and chemical reactions. The resulting network structure could possess distinct qualities, such as increased mechanical strength, water resistance, and biocompatibility.

By creating hydrogen bonds between the hydroxyl groups of PVA and the carboxyl and amine groups of CMC and chitosan, respectively, a physical network is formed. Depending on the circumstances, this kind of network development might be reversible and would not entail any covalent bonding **[27].**

1.7.   Scope of Study

Pakistan, which formerly had a water surplus, now has a water shortage. The amount of water per person has declined from 1,299 m3 in 1996–1997 to 1,100 m3 in 2006, and by 2025, it is expected to be less than 700 m3 per person. Only 1% of the home and industrial wastewater is treated in Pakistan. In order to reuse water and make Pakistan a water surplus country, industrial effluent must be treated in order to address the country's wastewater shortage.

- The project is significant because it makes use of chemically modified CMC, which is biocompatible, biodegradable, and stable in the environment. It also has a lot of potential as cost effectiveness, very efficient adsorbent for the removal of dyes.
- The project's primary relevance is the use of sustainable, promising, and renewable feedstock for water purification.
- We offer a unique and effective approach for synthesizing and characterizing CMC and chitosan-based nanocomposites in this research. We incorporated CMC, an anionic polysaccharide, together with CS to build a blended polymer network and also nanoparticles into it for making the hydrogel matrix more selective for one type of dye. The capacity of the nanocomposites to adsorb cationic and anionic dyes such as MB, MO, and CV was examined. Because chitosan and CMC are cellulose derivatives, which are plentiful natural polysaccharides, this method is termed green synthesis. [14].

CHAPTER 2

2. Literature Review

Tanzifi, Yaraki et al synthesized polypyrrole/CMC nanocomposite particles and used to remove the very hazardous dyes RR56, and RB160. The amount of CMC proved to be highly effective on surface adsorption effectiveness. To optimize the effect of variety of factors such as initial dye concentration, pH, adsorption period, and adsorbent dose were utilized. The highest adsorption of RB160 and RR56 was discovered under optimized conditions: adsorption period of 55 minutes and 52 minutes for RR56 and RB160, respectively, pH 4 and 5, initial dye concentration of 100 mg/L, and catalyst dosage of 0.09 g for each dyes. The created nanocomposite demonstrated significant reusability up to three batch adsorption cycles. [28]

Abou Taleb, Abd El-Mohdy et al. PVA and CMC copolymer hydrogels were created using an electron beam as a crosslinking agent. The copolymers were characterised using FTIR and mechanical characteristics such as gelation. The thermal sensitivity and swelling capabilities of the hydrogels formed were investigated in relation to the PVA/CMC ratio. The effects of CMC content, pH, initial concentration, and sorption temperature for dyes on acid, reactive, and direct dye adsorption capability onto PVA/CMC hydrogel were investigated. Thermodynamic research found that the adsorption process is exothermic because of the negative values of H. H (38.81 kJ/mol) suggested that electrostatic force was the predominant cause of dye adsorption [29].

Radoor, Karayil et al. developed a unique PVA/CMC/halloysite nano clay film for the efficient adsorption of MB (cationic dye) from aqueous environments. Under optimum conditions, such as

a nano clay dose of 6%, an initial dye concentration of 10 ppm, a contact period of 240 minutes, a pH of 10, and a temperature of 30 °C, the membrane has an amazing removal effectiveness of 99.5 percent for MB. Desorption studies demonstrated that the membrane can still be reused after four recycles [27].

He, Jia et al generated a natural healing luminous hydrogel based on oxidised CMC with outstanding Ag+ sensitivity and adsorption properties. The effects of hydrogel sensing and adsorption on heavy mineral ions were examined. With a detection limit of 3.798 M and a maximum capacity for adsorption of 407 mg/g, the fluorescent hydrogel displayed accurate detection as well as significant adsorption capacity for Ag+. The hydrogel may self-heal and be easily replicated seven times without losing its adsorption efficiency. In summary, the ability of the generated hydrogel to self-heal, detect and adsorb ions of heavy metals concurrently, and have high mechanical strength made it an excellent long-life adsorbent and proposed a new way for the treatment of wastewater [30].

López-Valdivieso, Lozano-Ledesma et al. studied CMC adsorption on galena (PbS) using electrokinetic, adsorption, and ATR-FTIR spectroscopy. Furthermore, The adsorption of CMC on CuFeS2 was compared to PbS. Adsorption of ethyl xanthate on PbS is more accurate than adsorption of CMC. When SO4 species are formed on the PbS surface as a result of oxidation, they promote CMC co-adsorption, leading the PbS surface to become hydrophilic in addition to the hydrophobicity caused by adsorbed ethyl xanthate. During oxidation, CMC considerably reduced the high level of PbS floatability while leaving CuFeS2 floatability alone. The use of non-toxic CMC as a PbS inhibitor in the extraction of Pb-Cu aggregate deposits while floating CuFeS2 was studied [31].

Jin, Xu et al described the creation of a novel MOF-5-CMC adsorbent capable of extracting the ions of lead from water-based solutions. We studied the influence of contact time, pH, initial Pb(II) concentration of the solution, and adsorption temperature on adsorption capacity. The adsorption ability of MOF-5-CMC beads is good; the greatest adsorption rate determined from the Langmuir isotherm-model is 322.58 mg/g, and adsorption equilibria is attained in a period of 120 minutes at a concentration of 300 mg/L. He concluded that MOF-5-CMC is an excellent adsorbent for removing Pb(II) from aqueous solutions [32].

Ding, Yi et al did modification of Na-CMC by oxidizing agent H_2O_2 to increase its solid content because DCMC has low concentration of solid material which reduces its commercial applications. Pre-degraded Na-CMC was synthesized by dissolving Na-CMC in DI water and the added 6% of Cu-Fe catalyst. After that 1.5ml of H_2O_2 was added into the solution and the reaction was continued for 10-15 min at 30°C. Again Na-CMC and H_2O_2 in same amount was added into the mixture in sequence and reaction continued for 110 min at 30°C. So, HCMC with 10% solid content was obtained. Further oxidization of HCMC was done by sodium periodate by conventional method. The solid content of oxidized CMC might be increased to about 30% under ideal circumstances. With the help of this DCMC, leather that has just been tanned might have high shrinkage temperatures and good fibre dispersion. Additionally, leather tanned with DCMC displayed similar physical and organoleptic qualities to leather tanned with commercial polyaldehyde tanning agent TWT and chrome tanning agent. This suggests that DCMC with a high content of solids could be a useful tanning agent [33].

Dou, Zhang et al developed edible DCMC films that were crosslinked with glycerol plasticized feather keratin films. DCMC was synthesized by mixing 4g of CMC in 80ml DI water in a beaker

for 12h. then added 40ml of 0.11g/mL of periodate solution. Reaction was carried out in dark environment and pH was maintained to 3.0 by HCl. The product was precipitated out by excess of ethanol and then washed and dried. The composite film FK/DCMC was prepared by casting method. On light dissemination, aggregate structure, tensile properties, permeability to water, and water vapor barrier on the microstructure the impact of DCMC crosslinking was examined. According to the findings, FK and DCMC formed covalent and hydrogen bonds, resulting in amorphous films of DCMC/FK with good UV-barrier characteristics and transparency. A slight decrease in the amount of moisture, solubility, and water vapour permeability revealed that DCMC crosslinking reduced the sensitivity of the FK films to moisture. As a result, DCMC crosslinking improved the FK films' potential viability for applications in food packaging and provided a value-added good [34].

Kulikowska, Wasiak et al presented two different methods of oxidation of CMC, one by using NaIO$_4$ oxidizing agent and the other by using hydrogen peroxide in which iron FePcS is used as catalyst. The oxidation of CMC by using sodium periodate is based on breakage of C$_2$_C$_3$ bond of glucose unit and forms two aldehyde groups per glucose unit. The oxidation of CMC by using hydrogen peroxide in the presence of catalyst is based on breakage of C$_2$_C$_3$ bond of vicinal diols of glycoside units. It introduced the carboxyl and carbonyl functionalities along the polysaccharides. This modified CMC is then used in nanoparticles preparation in medical diagnostics [35].

Li, Wu et al transformed CMC to its dialdehyde derivatives by periodate oxidation in acidic solution was given, and the effects of reaction time, periodate dosage, pH, and temperature were investigated. He postulated an acid-catalyzed cleavage mechanism for the -1-4-glycosidic

bond. His research estimates the considerable breakdown in the periodate oxidation procedure for derivatizing cellulose, which is important for discovering novel carboxymethyl polysaccharide derivatives [36].

Ogushi, Sakai et al used aqueous phase carbodiimide activation chemistry to introduce phenol moieties into carboxymethylcellulose by covalently introducing tyramine in carboxymethylcellulose. The resultant hydrogel was created by utilizing H_2O_2 as an oxidizing agent in a peroxidase-catalyzed oxidation process of phenol. After 24 hours, the hydrogel formed from 1.5% (w/v) conjugated solution, 5 units/ml horseradish peroxidase, and 1 mM H2O2 retained 80% of the vitality of the inner mammalian cells. These findings highlight the potential of this CMC with phenol components for biomedical applications such as tissue engineering [37].

Sharma, Kaith et al synthesized biocompatible and biodegradable Gelatin, dialdehyde carboxymethyl cellulose and dextrin based dialdehyde hydrogels which have a very important role in biomedical field. Oxidation of CMC was done by adding 1g CMC in 100ml distilled water and the added 6% w/v of sodium periodate into and reaction was carried out in under dark environment. The oxidation reaction was stopped by ethylene glycol by adding 3-4 drops of it. To cross link the gelatin with oxidized dextrin and DCMC, glutaraldehyde is used as a cross linker and in this way introduced the imide bond that has a good self-healing property. The rheological studies showed that these cross-linked materials also have injectable properties because of low viscosity of hydrogels. The sample's biomedical significance was further underscored by the discovery that it is blood compatible [38].

Shen, Li et al prepared shiff base reaction between oxidised CMC with DTP yielded pH and oxidation dual stimuli-responsive injectable hydrogels. CMC was oxidised by mixing 24ml of 6.7%w/v sodium periodate into 2g of CMC dissolved in 250ml DI water, and the reaction was then carried out in a dark setting at room temperature. Different concentrations of oxi-CMC were mixed with different concentrations of DPT solutions to synthesize the series of OCMC/DPT hydrogels which are an attractive candidate for Material for a medication delivery system, transplantation, or cell scaffoldings [39].

Hivechi, Joghataei et al synthesized in situ gelling hydrogels by OCMC and gelatin to heal diabetic wounds. Strätz et al. approach was used to prepare the OCMC, and the hydrogel was created by mixing OCMC and gelatinous solutions in two 10ml syringes, which were then put into a Harvard Instrument Pump 11 Elite and linked to a self-designed rubber coaxial mixing nozzle. The final step was the lyophilization of produced hydrogel. This hydrogel keeps the wound moist since it can absorb nearly 10 times its weight. According to the results, the OCMC-Gel hydrogel was found to be able to speed up the healing process in both diabetes and non-diabetic wounds [40].

Yu, Weng et al focused-on preparation of DCMC and its cross-linking with collagen fibril hydrogel (CH). He explained two modes of cross-linking of DCMC to CH 'multiple or short range' and 'limited and long-range cross linking. The DCMC was produced using Teotia and Mu's approach, with some modifications. According to the findings, DCMC having % -CHO improved the physical and chemical features of CH by establishing sufficient Schiff-base couplings with collagen filament across a relatively short distance. To put it another way, by altering its -CHO

amount and molecular weight, DCMC has the ability to satisfy the need for protein-based products

with various expectations [41].

CHAPTER 3

3. <u>EXPERIMENTAL DETAILS</u>

3.1.   Materials

Carboxymethyl cellulose (CMC) and Sodium periodate (≥99.8%), were purchased from Sigma–Al drich®. Chitosan (200-400mPa.s) was purchased from Macklin, SiC nanoparticles, CTAB, TEOS, NH_4OH, acetic acid, HCl, NaOH, $AgNO_3$.

3.2.   Apparatus and Instruments

Hot plate stirrer, magnetic bar, flasks, beakers, spatula, sucker, pipette, pH strips, vials, Eppendorf, plastic and glass petri dishes, centrifuge tubes, centrifuge machine, weighing balance, FTIR, SEM, XRD, tensiometer, and TGA analyzer for analysis and characterization.

3.3. Methodology

3.3.1. Oxidation of CMC by using $NaIO_4$ Oxidizing agent

The oxidized Carboxymethyl cellulose by oxidation was prepared as follows: 3g of CMC was mixed in 10ml deionized water in round bottom flask that has magnetic stirrer in it and was placed in oil bath. Then added solution of 4.5 g $NaIO_4$ in CMC solution under constant stirring in the dark conditions. The pH up to 3 was adjusted by 1M H_2SO_4. After mixture was stirred for 4 hours, excess of ethanol was poured into the solution and stand it overnight to precipitate out the oxidized product. Then centrifuged the solution to separate out the product and then product was washed and dried.
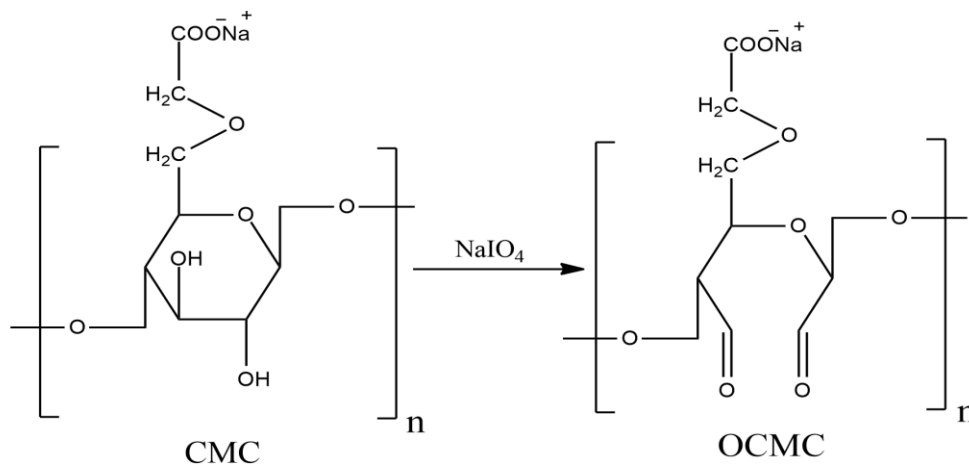
Figure 3.1. Oxidation reaction of CMC in the presence of NaIO₄

3.3.2. Reaction of OCMC with CS

Different amounts of OCMC (0.3 ,0.4, 0.5) were stirred with fixed quantity of chitosan i.e 0.5g in 4% solution of acetic acid to prepare different weight ratio of OCMC-CS films. After the addition of chitosan, the solution was stirred overnight to maximize the chances of crosslinking. Then did filtration of mixture and dried the filtrate. Yellow colored shiff base is formed.
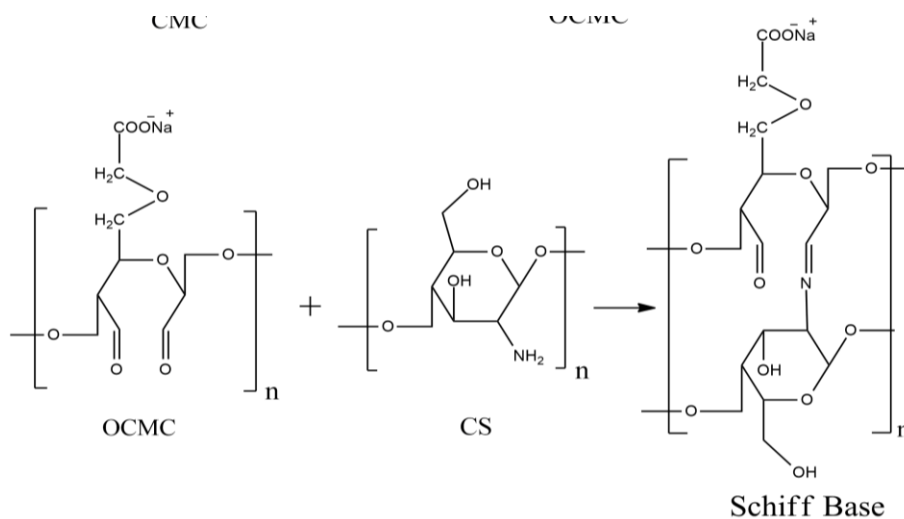

Figure 3.2. Reaction between OCMC and CS to form Shiff Base

3.3.3. Synthesis of silica coated silicon carbide nanoparticles (SiC@SiO₂)

The adaptable solution sol-gel approach was used to create SiC@SiO2 microspheres. The already synthesized SiC nanoparticles (0.4 g) were well disseminated in a conical flask containing water (20 mL), CTAB (0.6 g), and concentrated NH4OH (8.0 mL). Following dispersion, 0.8 g of TEOS was added dropwise to the reaction, which was allowed to proceed for 12 hours with constant mechanical stirring. The resultant product was rinsed with distilled water and ethanol (1:1), and the silica coated silicon carbide nanoparticles were allowed to air dry at 50 degrees Celsius for 24 hours.

3.4. Preparation of Films

3.4.1. Carboxymethyl cellulose (CMC) film preparation

700 mg of pure CMC was dissolved in 1% acetone solution to prepare CMC membrane and 30% w/v PVA is added into it as a binder. The homogenous mixture was casted into round plastic petri dish. The membrane was subsequently allowed to dry in air.

3.4.2. CMC-SiC -20 nanocomposite film

700 mg of pure CMC was dissolved in 1% acetone solution and then added 20% w/v of SiC nanoparticles by stirring. 30% w/v PVA is added into it as a binder. The homogenous mixture was casted into round plastic petri dish. The membrane was subsequently allowed to dry in air.

3.4.3. CMC-SiC@SiO₂-10,15,20 nanocomposite films

700 mg of pure CMC was dissolved in 1% acetone solution and then added 5%, 10%, 15% and 20% SiC/SiO2 nanoparticles into it and allowed stirring until homogenized mixture found. Then

added 30% w/v PVA is added into it to increase its mechanical strength. The homogenous mixture was casted into round plastic petri dish. The membrane was subsequently allowed to dry in air.

3.4.4. Film of Pure CS

700 mg of pure CS was dissolved in 1% solution of acetic acid to prepare film of chitosan. The homogenous mixture was casted into round plastic petri dish. The film was subsequently allowed to dry in air. After drying, the solution of NaOH was used to wash the films to neutralize the effect of acetic acid. After washing several times with distilled water, the film was allowed to dry on the same petri dish at room temperature.

3.4.5. CS-SiC-20 nanocomposite film

700 mg of pure CS was dissolved in 1% solution of acetic acid and then added 20% w/v of SiC nanoparticles by stirring. The homogenous mixture was casted into round plastic petri dish. The film was subsequently allowed to dry in air. After drying, the solution of NaOH was used to wash the films to neutralize the effect of acetic acid. The film was dried on the same petri plate at room temperature after being washed many times with distilled water.

3.4.6. CS-SiC@SiO$_2$-10 nanocomposite film

700 mg of pure CS was dissolved in 1% solution of acetic acid and then added 10%, 15% and 20% SiC@SiO$_2$ nanoparticles into it and allowed stirring until homogenized mixture found. The homogenous mixture was casted into round plastic petri dish. The membrane was subsequently allowed to dry in air. After drying, the solution of NaOH was used to wash the films to neutralize the effect of acetic acid. The film was dried on the same petri plate at room temperature after being washed many times with distilled water.

3.4.7. Preparation of OCMC-CS film

1:1 OCMC was mixed with CS in 3% solution of acetic acid to prepare OCMC-CS film and then did overnight stirring. Then added 30% of PVA into it as a binder. The homogenous mixture was casted into round plastic petri dish. The film was subsequently allowed to dry in the air. Following drying, the membrane was rinsed with a NaOH solution, followed by distilled water, to remove non-cross-linked groups of aldehyde and imine linkages between OCMC and CS and to neutralize the action of acetic acid. The film was dried on the same petri plate at room temperature after being washed many times with distilled water.

3.4.8. Preparation of OCMC-CS-SiC-20 nanocomposite film

1:1 OCMC was mixed with CS in 3% Acetic acid solution and then did overnight stirring. After that, 20% of SiC nanoparticles were added into it and allowed stirring until homogenized mixture found. Then added 30% of PVA into it as a binder. The homogenous mixture was casted into round plastic petri dish. The film was subsequently allowed to dry in the air. Following drying, the membrane was rinsed with a NaOH solution, followed by distilled water, to remove non-cross-linked groups of aldehyde and imine linkages between OCMC and CS and to neutralize the action of acetic acid. The film was dried on the same petri plate at room temperature after being washed many times with distilled water.

3.4.9. Preparation of OCMC-CS-SiC@SiO$_2$-10,15,20 nanocomposite films

1:1 OCMC was mixed with chitosan in 3% Acetic acid and then did overnight stirring. After that, 10%, 15% and 20% added SiC@SiO$_2$ nanoparticles into it and allowed stirring until homogenized mixture found. Then added 30% of PVA into it as a binder. The homogenous mixture was cast into round plastic petri dish. The film was subsequently allowed to dry in air. Following drying,

the membrane was rinsed with a NaOH solution, followed by distilled water, to remove non-cross-linked groups of aldehyde and imine linkages between OCMC and CS and to neutralize the action of acetic acid. The film was dried on the same petri plate at room temperature after being washed many times with distilled water.
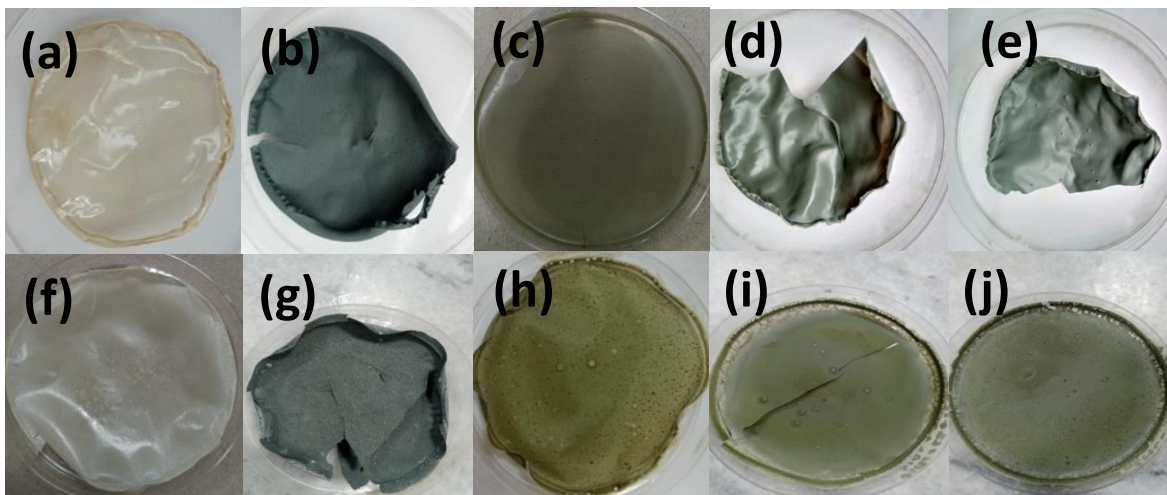

Figure 3.3. Digital Film Images of CS (a), CS-SiC-10 (b), CS-SiC@SiO2-20 (c), CS-SiC@SiO2-15 (d), CS-SiC@SiO2-20 (e), OCMC-CS (f), OCMC-CS-SiC-20 (g), OCMC-CS-SiC@SiO2-10 (h), OCMC-CS-SiC@SiO2-15 (i), OCMC-CS-SiC@SiO2-20 (j)

CHAPTER 4

4. RESULTS AND DISCUSSIONS

4.1. Characterization

In this chapter, the characterization of starting material CMC, OCMC, OCMC-CS, and nanoparticles are explained in detail. The main characterization techniques employed are:

- ➢ FTIR
- ➢ SEM
- ➢ XRD
- ➢ TGA

4.1.1. XRD Analysis

XRD is a flexible, non-destructive analytical method that is used to examine crystalline materials. This method enables the investigation of the material's structure, including the size, d-spacing, and atom arrangement of the crystallites. Crystalline samples are affected by monochromatic x-ray interactions in XRD analysis. A cathode ray tube produces an X-ray beam by heating the filament. These x-rays are then focused on the object to be studied after passing through a monochromator to create monochromatic x-rays. X-rays target the substance, reflect, and are then detected by the detector, processed, and transformed into signals. The Scherer equation can be applied to XRD data to determine the size of the crystallite. [42]

The SiO_2 shells on the SiC core were confirmed by an XRD test, and the resulting band diffraction peaks of untreated and treated SiC nanoparticles are shown in Fig. 4.1 The existence of amorphous

SiO2 is clearly demonstrated by the wide and broad peak at 2θ = 21°. SiC is attributed to the diffractions at 2θ = 35.6, 41.3, 60.0, and 71.8°. When thermally oxidized, the intensity of the major SiC peak at 35.6° decreased, demonstrating that the amount of SiC was decreased. A broad peak of Fig. 4.2 at angle 2Θ = 21.24◦ has confirmed the amorphous nature of polymers. The silica coating on SiC nanoparticles is very thin that's why not prominent peak appeared for SiO_2 [43].
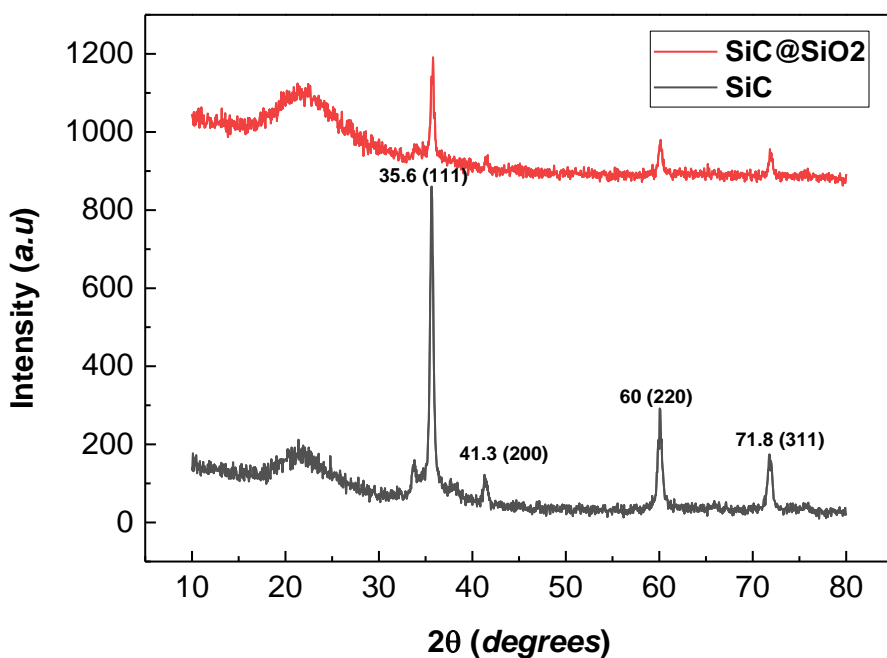

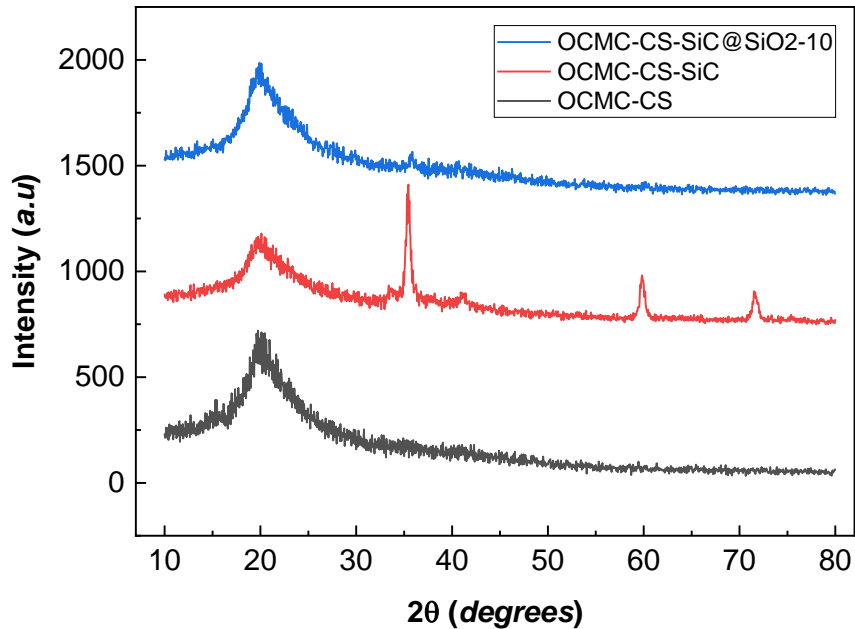*Figure 4.1. XRD Analysis of SiC nanoparticles and SiC@SiO₂ nanoparticles*

Figure 4.2. XRD Analysis of OCMC-CS, OCMC-CS-SiC, OCMC-CS-SiC@SiO$_2$-10

4.1.2. Fourier transform infrared spectroscopy (FTIR)

FTIR provides information about the functional characteristics that connect the functional group and the structure of the composite blended film. By transitioning electrons in the same electronic shell from a lower vibrational level to a higher vibrational level, organic compounds and some inorganic compounds can produce stretching and bending vibrations when exposed to electromagnetic radiation in the IR area between 4000 cm-1 and 400 cm-1 (2.5 m to 25 m). Bonds' changing dipole moments are what cause the vibrations that show up in IR spectra. [44]

According to Fig. 4.3, a large peak at 3350 cm1 corresponds to polymer O-H stretching. The overlapped peak of a carboxyl group from CMC and amine bond of CS is ascribed to 1597 cm1. The C-H bending of CMC is responsible for the peak at 1333 cm1 [17]. The steep rise at 1068 cm1

is due to the C-O stretching of the CMC and CS polymer skeletons. The peak at 809 cm-1 represents the Si-C stretching vibration mode of SiC. Stretching vibrations due to the presence of -CH3 are visible at 2925 cm-1, with unsaturated C-H stretch about 3000 cm-1. The peak at 1715 represents the C=O of aldehyde. The C-O-C stretching vibration is 1070 [45].

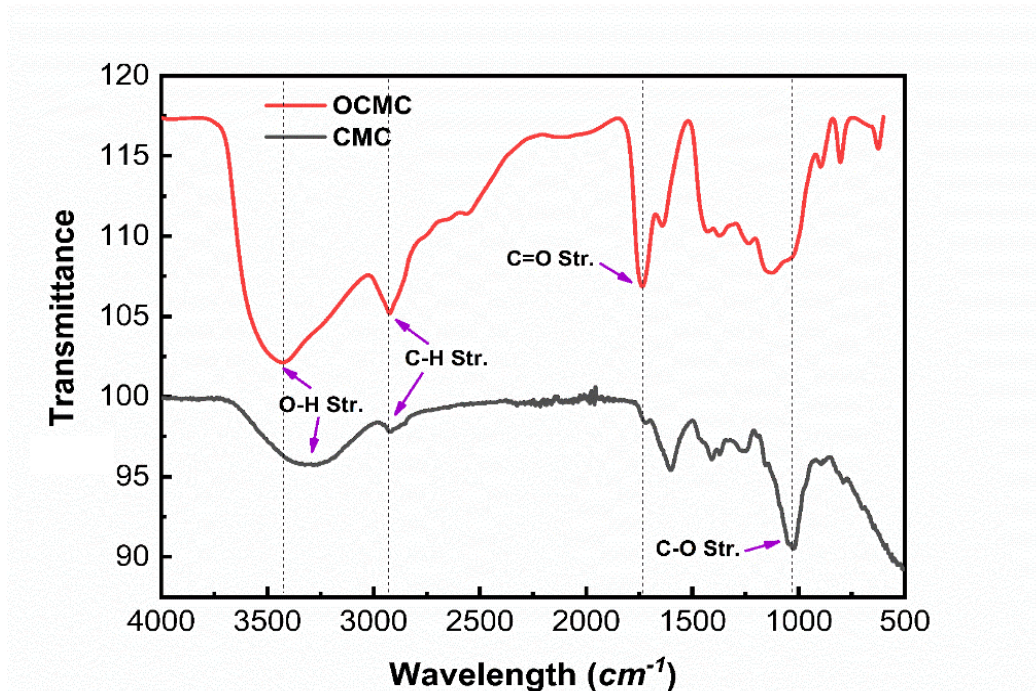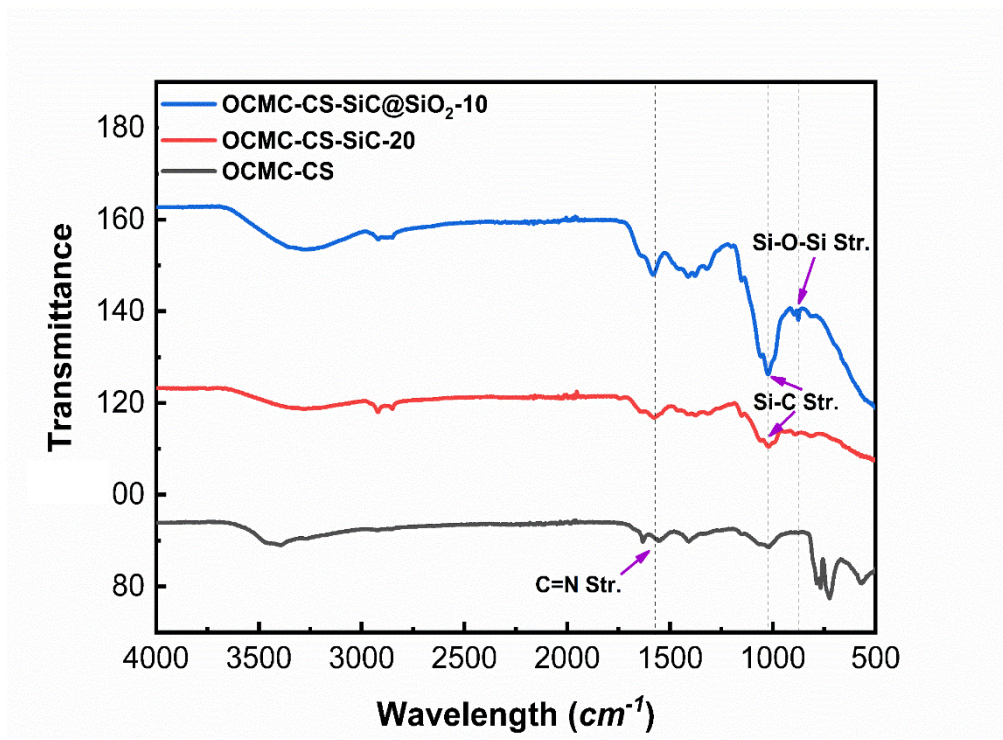*Figure 4.3. FTIR analysis of CMC, and OCMC*

Figure 4.4. FTIR analysis of OCMC-CS, OCMC-CS-SiC-20, and OCMC-CS-SiC@SiO₂ -10

4.1.3. TGA Analysis

TGA was used to examine the changes in thermal stability of OCMC-CS and its nanocomposites with SiC and SiC@SiO2. Fig. 4.5, 4.6, 4.7 depicts the TGA and DSC curves of OCMC-CS, OCMC-CS-SiC-20, and OCMC-CS-SiC@SiO2-10 respectively. According to the TGA curve, there are three thermal events that occur during the degradation of OCMC-CS, OCMC-CS-SiC-20, and OCMC-CS-SiC@SiO2-10: first, dehydration occurs in 80-250°C temp. range, resulting in weight losses of 13.37%, 11.22%, and 11.63% of the total weight, respectively; second, there is a uniform and smooth decline in weight loss in the temperature range of 250-400°C. After this, the glucose units in the structure are destroyed leading towards the final degradation of the polymer at 450 °C and the residual mass of OCMC-CS, OCMC-CS-SiC-20 and OCMC-CS-SiC@SiO₂-10 after degradation is 29.08%, 40%, 30.9% respectively.

The TGA and DSC curve of OCMC-CS and its nanocomposites with SiC and SiC@SiO$_2$ as compared with the OCMC-CS without nanoparticles are thermally more stable. This detailed thermal analysis can be helpful for further studies and applications.
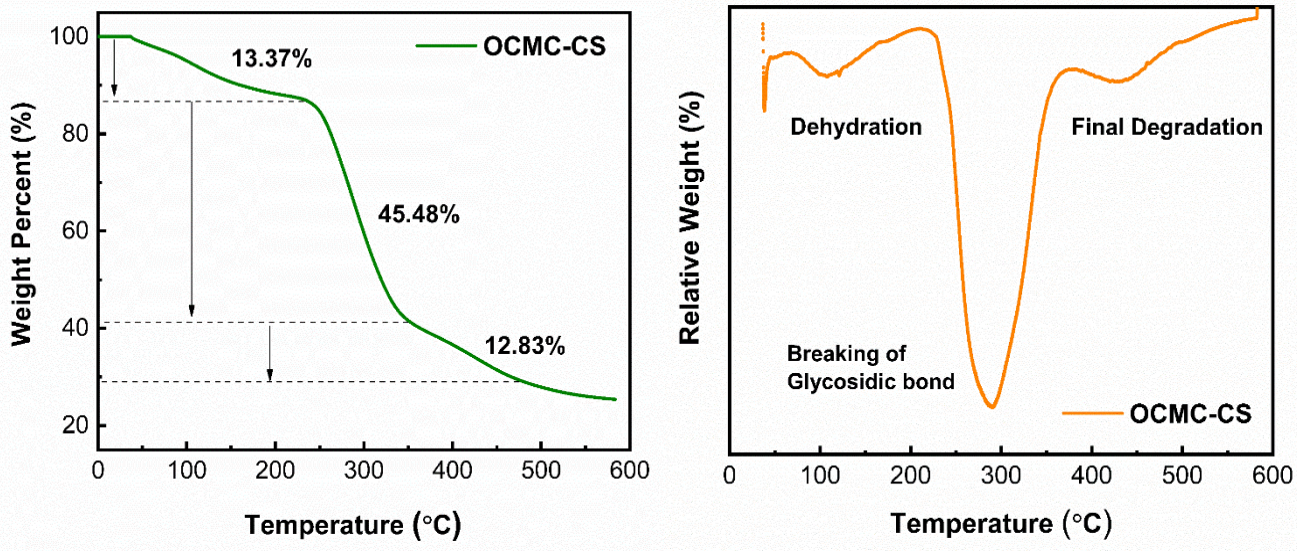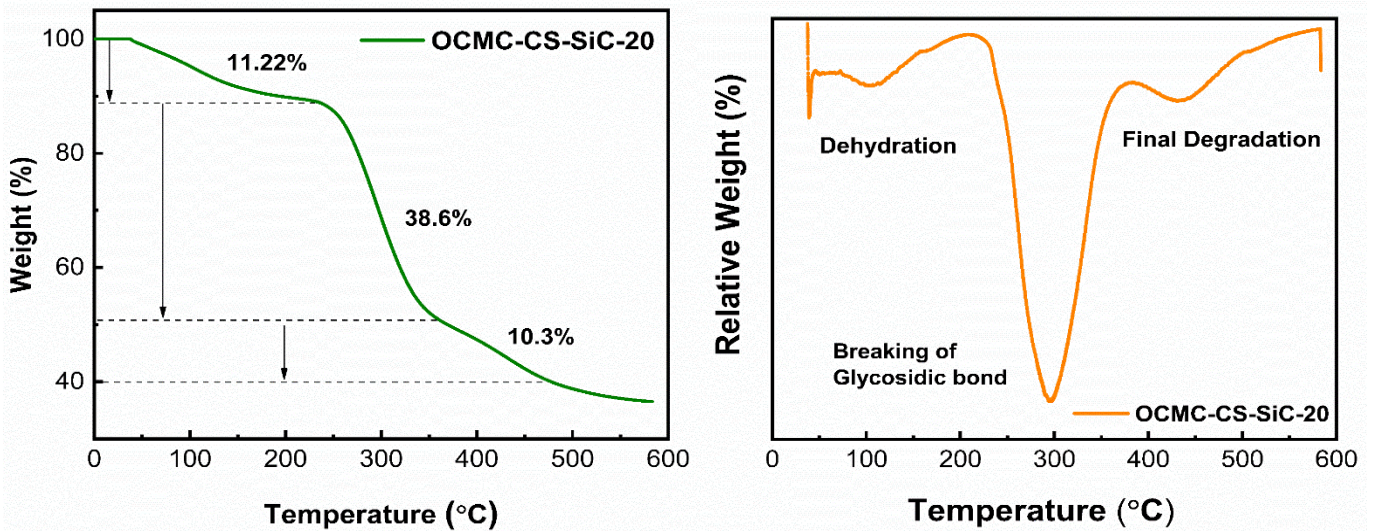

Figure 4.5. TGA and DSC of OCMC-CS

Figure 4.6. TGA and DSC of OCMC-CS-SiC-20
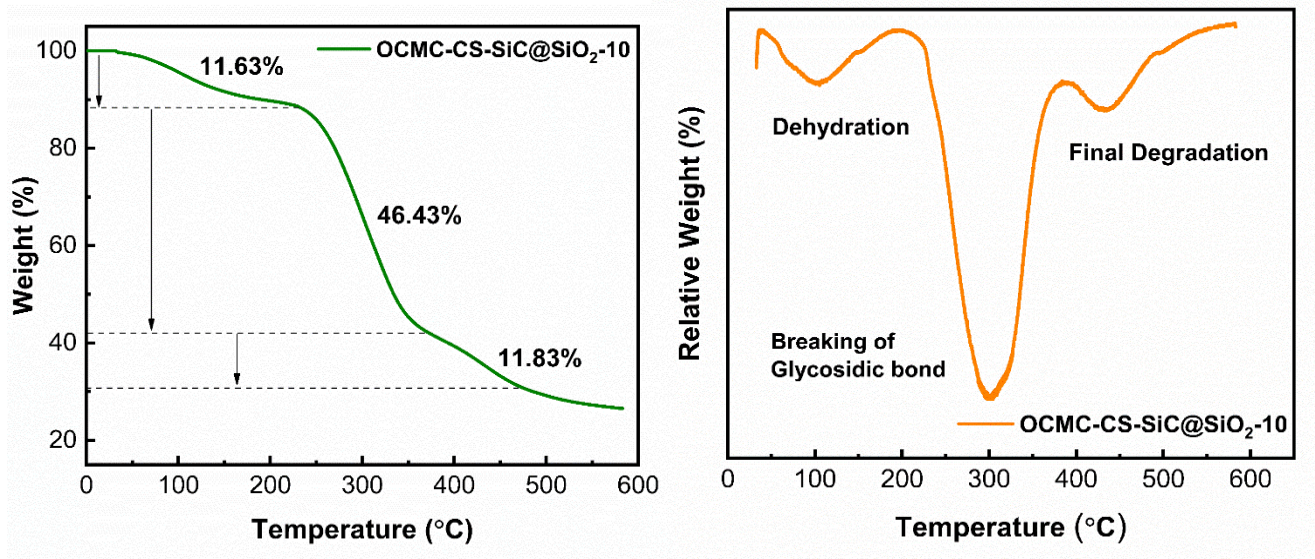
Figure 4.7. TGA and DSC of OCMC-CS-SiC@SiO₂-10

Polymer	Temperature (°C)	Residual Mass (%)
OCMC-CS	290.95	29.08
OCMC-CS-SiC-20	298.76	40
OCMC-CS-SiC@SiO₂ -10	301	30.9

Table 4.1. Degradation Temperature and Residual Mass (%) of OCMC-CS, OSMS-CS-SiC-20 and OCMC-CS-SiC@SiO2-10

4.1.4. SEM Analysis

The surface morphology of synthesized material is analyzed by scanning electron microscopy. From Fig. 4.8, morphology analysis of OCMC-CS shows high porosity as the pores are well-distributed and continuous. OCMC-CS-SiC-20 decreases the porosity as nanoparticles are incorporated in pores and OCMC-CS-SiC@SiO₂-10 further reduces the porosity.

Fig. 4.8 (a) shows that there are interconnected channels of OCMC-CS and the porosity. These white spots may be because of aggregation of polymers due to C=N linkages. Fig. 4.8 (b) shows that SiC nanoparticles are incorporated in channels and pores of OCMC-CS due to which porosity decreased. Fig. 4.8 (c) shows that there is further decrease in porosity because of SiC@SiO$_2$ nanoparticles incorporation. Fig. 4.9 shows the SEM image of OCMC-CS after adsorption. The dark area shows that the MB dye molecules are adsorbed on the surface of adsorbent.

The elemental analysis of synthesized material is performed using EDX. In its own composition, nanocomposite contains carbon (C), oxygen (O), nitrogen (N), and silicon (Si). These results demonstrated that silica nanoparticles were successfully integrated into the film matrix. Furthermore, element mapping demonstrated that silica nanoparticles are distributed uniformly throughout the superabsorbent nanocomposite [46].

(a) Formula	mass%
C	47.57
N*	1.17
O	49.54
Na	1.72
Total	100.00

(b) Formula	mass%
C	38.21
N*	2.02
O	35.43
Na	6.06
Si	18.28
Total	100.00

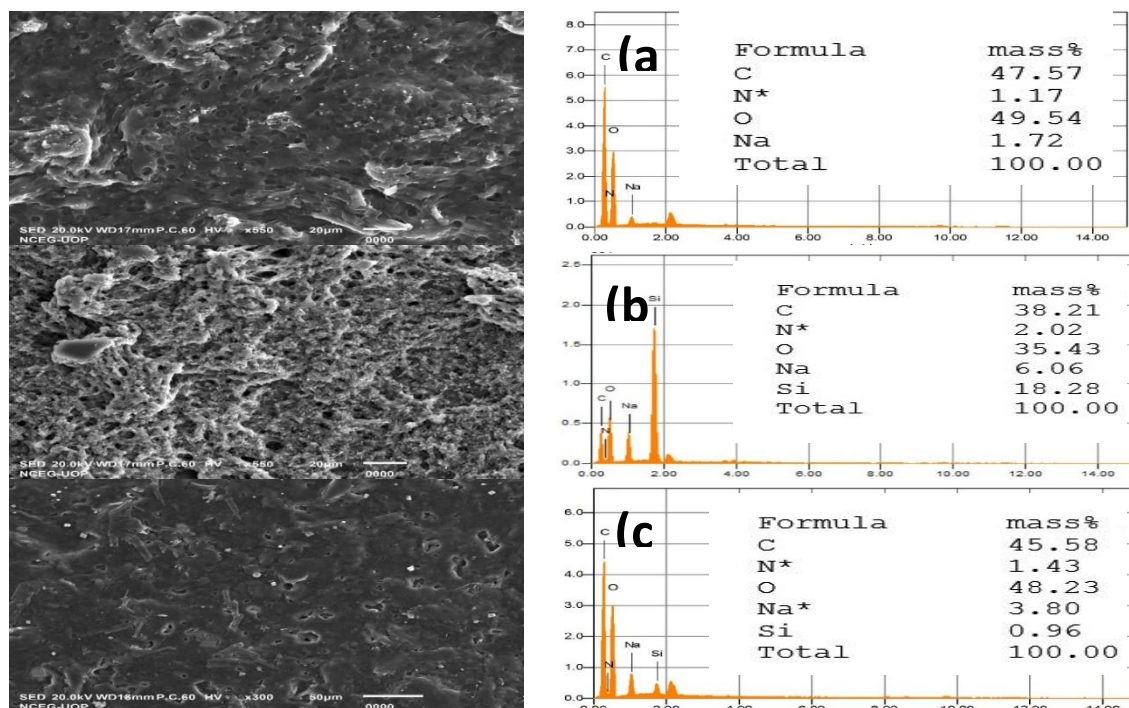| (c) Formula	mass%
C	45.58
N*	1.43
O	48.23
Na*	3.80
Si	0.96
Total	100.00

Figure 4.8. SEM images and EDX of OCMC-CS (a), OCMC-CS-SiC-20 (b), OCMC-CS-SiC@SiO$_2$-10 (c)
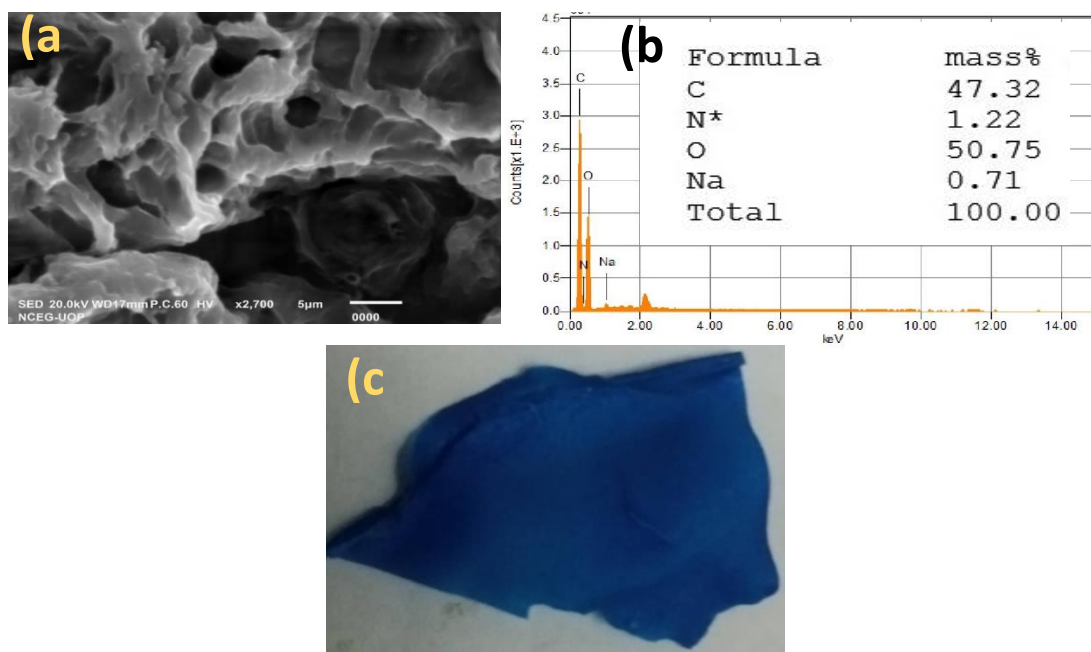
Figure 4.9. SEM images and EDX of OCMC-CS after adsorption

CHAPTER 5

5. APPLICATION

5.1. Dye Adsorption study

In the adsorption of MB, MO, CV dyes, the effects of contact time, catalyst dosages, initial dye concentration, pH, and temperature were investigated. One parameter was changed during the experiment while the other parameters kept constant. 30 mL bottles of dye solutions were used for the adsorption studies. 30mg of each membrane was placed in 30ml of each dye solution and then measured absorbance of each solution at 660nm, 465nm, 580nm for λ_{max} of MB, MO and CV respectively, against the parameters of pH, initial dye concentration, adsorbent dosage, contact time, and temperature in the range of 7, 0.05mM, 50-150mg, 30–150 min, and 10-70◦C, respectively. These tests were carried out using a UV-Visible spectrophotometer.

Because of the active sites on the surface of adsorbents and the high electrostatic interaction between the negatively charged adsorption materials and positively charged MB and CV dyes, MB and CV adsorption was initially quick. The adsorption slowed down with time until equilibrium was reached. MO is an anionic dye and there was not good adsorption of MO dye on the surface of adsorbents which shows that there is no adsorbate-adsorbent attraction.

5.2. Screening of different adsorbents against MB, MO, and CV dye

Thirty 100ml beakers were washed and dried completely. They were labelled as CS (a), CS-SiC-20 (b), CS-SiC@SiO$_2$-10 (c), CS-SiC@SiO$_2$-15 (d), CS-SiC@SiO$_2$-20 (e), OCMC-CS (f), OCMC-CS-SiC-20 (g), OCMC-CS-SiC@SiO$_2$-10 (h), OCMC-CS-SiC@SiO$_2$-15 (i), OCMC-CS-SiC@SiO$_2$-20 (j). A known volume (30mL) of each dye solution (MB, MO, CV) of 0.05mM concentration was added in each beaker. After this, 100 mg of each adsorbent was added in all beakers and covered each beaker with aluminum foil and allowed them to rest. Took reading of each solution after every 30 minutes for 150 min. by UV-Visible spectrophotometer. MB gave best results with absorbents as it is cationic dye and adsorbent surface is negatively charged so there is good adsorbate-adsorbent interaction. Among all the adsorbents, 3 adsorbents (OCMC-CS, OCMC-CS-SiC-20, OCMC-CS-SiC@SiO$_2$-10) showed maximum adsorption with cationic dyes, MB and CV. A bar graph was plotted between time(min) and % adsorption values. The results are shown in Fig. 5.1.
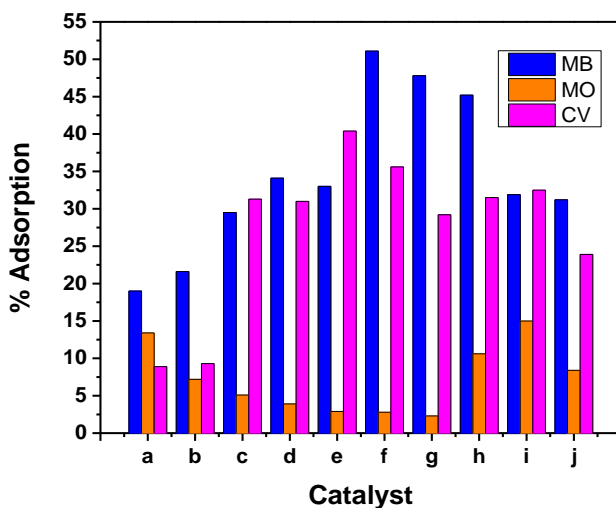

Figure 5.1 Screening of CS (a), CS-SiC-10 (b), CS-SiC@SiO2-20 (c), CS-SiC@SiO2-15 (d), CS-SiC@SiO2-20 (e), OCMC-CS (f), OCMC-CS-SiC-20 (g), OCMC-CS-SiC@SiO2-10 (h), OCMC-CS-SiC@SiO2-15 (i), OCMC-CS-SiC@SiO2-20 (j) with MB,MO,CV dyes

5.3. Calculations

The percentage removal (%R) and equilibrium adsorbed amount (q_e) of MB, MO, and CV dyes were calculated by using equation (5.1) and (5.2) respectively.

$$\%R = \left[\frac{Co - Ce}{Co}\right] \times 100 \tag{5.1}$$

$$q_e = \frac{[(Co - Ce)V]}{m} \tag{5.2}$$

where Co(mg/L) and Ce(mg/L) denote the starting and equilibrium concentrations. The volume of the solution is V (L), the mass of the samples is m (g), and the adsorption capacity is qe (mg/g).

5.4. Effect of Different Physical Parameters on the Adsorption Process

The following physical parameters were investigated to determine their impact on the adsorption process:

- Effect of Concentration
- Effect of Catalyst Dosages
- Effect of Contact Time
- Effect of pH
- Effect of Temperature

5.4.1. Effect of initial concentration

Different concentrations (0.05mM, 0.07mM and 0.09mM) of MB dye were studied under the following conditions: contact time of 150 min, 100mg of adsorbent at room temperature. From results, it is evident that the adsorption rate decreases with increase in concentration of dye solution because of saturation effect. At greater concentrations of the dye solution, it's possible that the adsorption sites on the polymer adsorbent become saturated. Initially, at lower concentrations, the polymer surface has a greater number of vacant adsorption sites, which results in a higher adsorption rate. The adsorption rate slows down, and the number of vacant sites declines as the concentration rises. All three adsorbents gave maximum adsorption with 0.05mM concentration of MB solution.

Experimental Condition: 100mg of each catalyst was treated against 30 mL of different concentration of dye solution for 150 minutes at room temperature and at pH 7.
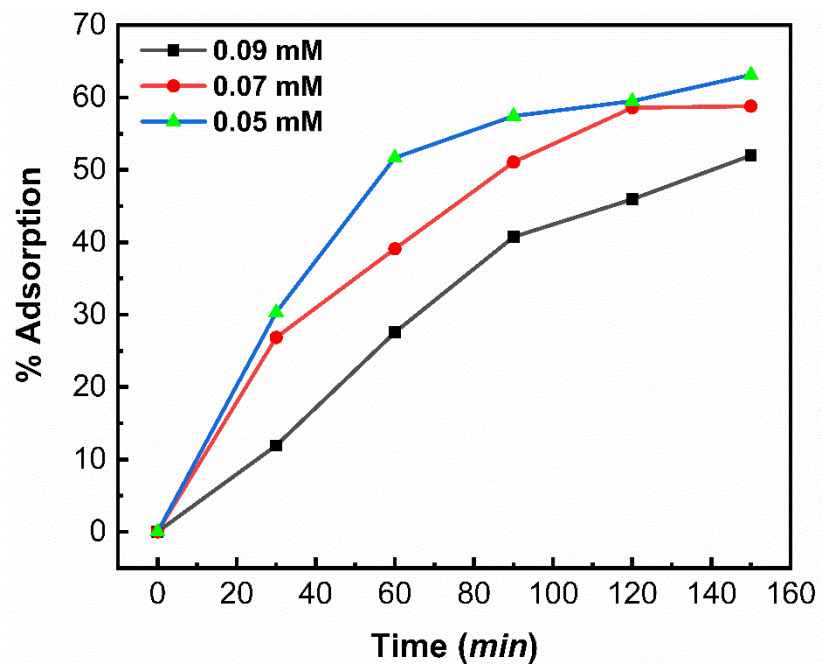
Figure 5.2. Effect of concentration of MB dye on the interaction of OCMC-CS

Time (min.)	0.09mM	0.07mM	0.05mM
0	0	0	0
30	11.92514	26.84767	30.32105
60	27.55559	39.10598	51.69441
90	40.74106	51.07121	57.43906
120	45.92502	58.57306	57.49851
150	51.99092	63.12403	58.79905

Table 5.1. % Adsorption of OCMC-CS at 0.05mM, 0.07mM, 0.09mM concentration of MB dye
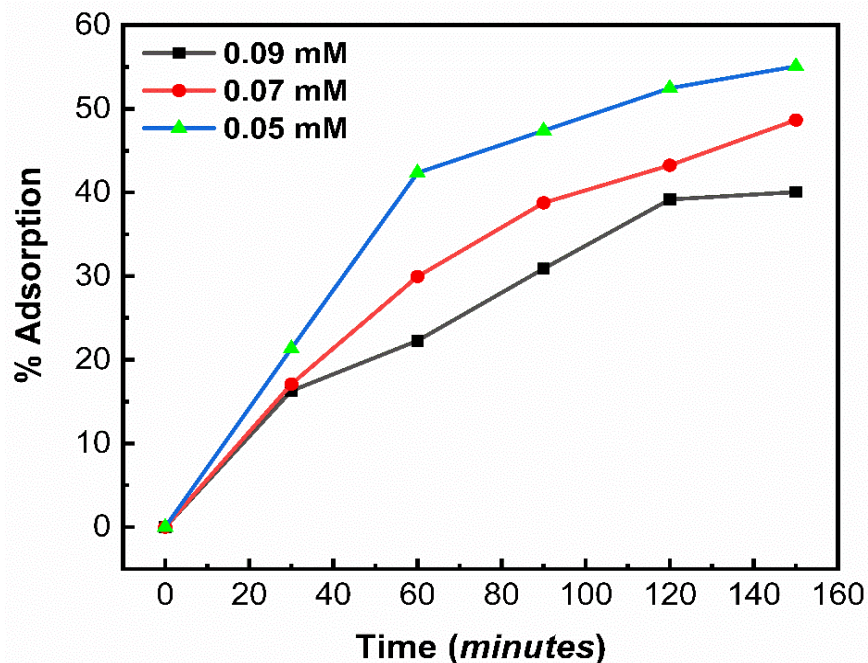
Figure 5.3. Effect of concentration of MB dye on the interaction of OCMC-CS-SiC-20

Time (min.)	0.09mM	0.07mM	0.05mM
0	0	0	0
30	16.288828	17.08886	21.33621
60	22.28432	29.95351	42.34542
90	30.88252	38.75564	47.3915
120	39.15182	43.24261	52.4673
150	40.04832	48.64583	55.0758

Table 5.2. Effect of concentration of MB dye on the interaction of OCMC-CS-SiC-20
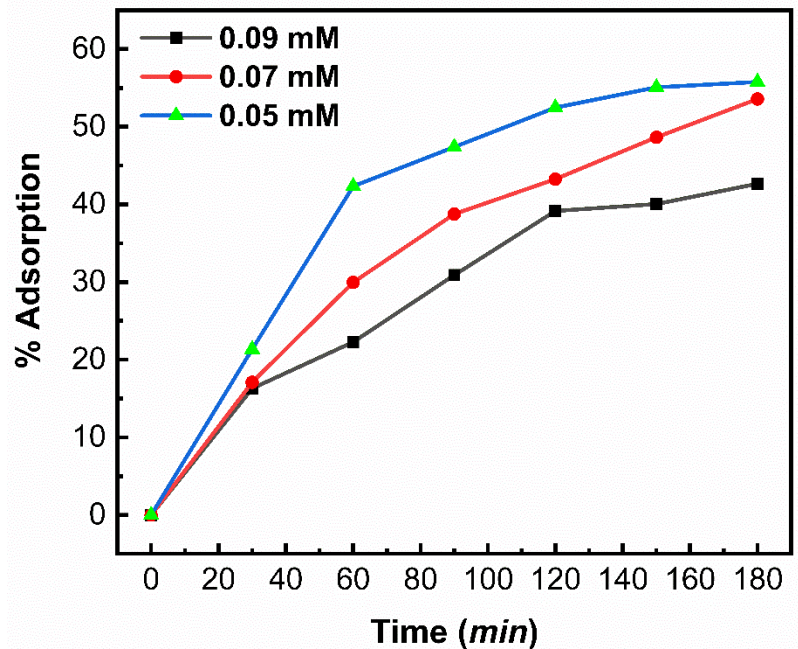
Figure 5.4. Effect of concentration of MB dye on the interaction of OCMC-CS-SiC-20

Time (min.)	0.09mM	0.07mM	0.05mM
0	0	0	0
30	18.0638	15.4012	27.95779
60	26.81046	27.79425	50.17093
90	34.04063	38.7927	50.67628
120	40.02212	46.27097	53.47057
150	45.90465	51.94031	58.38288

Table 5.3. % Adsorption of OCMC-CS-SiC-20 at 0.05mM, 0.07mM, 0.09mM concentration of MB dye

Adsorption Isotherms

The following equations of Langmuir (Eq. 5.3), Freundlich (Eq. 5.4) and Tempkin (Eq. 5.5) were used to analyze the experimental data.

$$\frac{C_e}{q_e} = \frac{1}{q_{max}} \times C_e + \frac{1}{k_L \times q_{max}} \qquad (5.3)$$

$$Ln(q_e) = \frac{1}{n} \times ln(C_e) + ln(k_F) \qquad (5.4)$$

$$q_e = \left(\frac{RT}{b_T}\right) lnA_T + \left(\frac{RT}{b_T}\right) lnC_e \qquad (5.5)$$

where qmax, kL,n, and kF and AT are the Langmuir, Freundlich, and Tempkin constants. qmax (mg/g), which denotes the maximum adsorption capacity, where KF denotes adsorption capacity and n denotes adsorption intensity. The universal gas constant is R (8.314 J/mol K), while the absolute temperature is T (K).

The Temkin constant (L/mg) refers to the highest binding energy, while bT (J/mol) denotes the heat of adsorption. All values were derived from the mathematical models' fit to the experimental data. The Langmuir, Freundlich, and Tempkin graphs for the adsorptions of MB onto OCMC-CS at 0.05mM, 0.07mM, and 0.09mM dye solution concentrations are shown in Fig 5.5. The Langmuir technique fitted the equilibrium data well, as shown in Fig. 5.5, with a high correlation coefficient (R^2), as stated in Table 5.4. It was discovered that the Langmuir model accurately described the

equilibrium adsorption data for MB adsorption because it had R^2 values closer to unity. The best mathematical adjustments to the Langmuir model show that MB adsorption on OCMC-CS occurs mostly through the chemisorption process, in which an adsorbate monolayer accumulates on the surface of the OCMC-CS. A higher KL value indicates more interaction between the adsorbent and adsorbate.
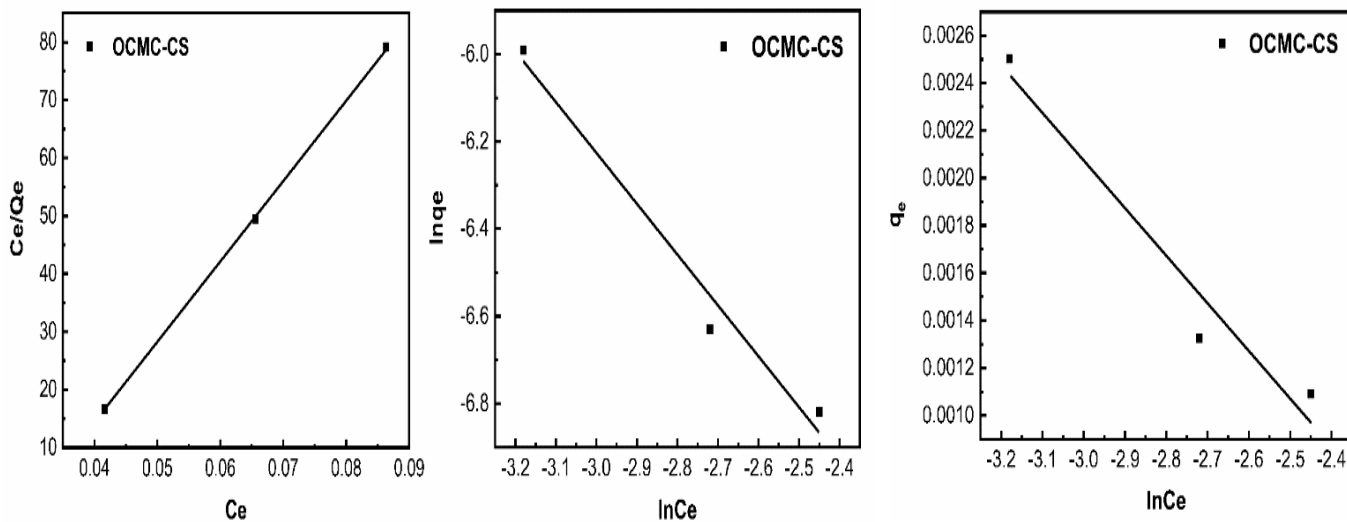
Figure 5.5 Adsorption isotherms (Langmuir, Freundlich, and Temkin) of MB for OCMC-CS

Langmuir		Freundlich		Tempkin	
KL	R^2	KF	R^2	KT (L mg-1)	R^2
2.5×10^{-3}	0.99673	6.23864×10^{-7}	0.89343	141029.8967	0.8365

Table 5.4 Isothermal parameters for the Langmuir, Freundlich and Tempkin models of OCMC-CS

5.4.2. Effect of contact time

3 beakers of 100 mL were washed and dried completely. They were labelled as OCMC-CS, OCMC-CS-SiC-20, OCMC-CS-SiC@SiO$_2$-10. A 30ml volume of 0.05mM MB solution was added in each beaker. After this, 30mg of each adsorbent was added in different beakers at the same time and allowed them to rest. Took reading of each solution after every 30 minutes for 150 minutes by UV-Visible spectrophotometer. A graph was plotted between time of contact (min) and % adsorption. The results showed that adsorption increases with time and 150 minutes is equilibrium time. The quick initial increase in the quantity of adsorbed dye may be related to an increase in the quantity of accessible unoccupied sites at the start, and equilibrium is reached at 150 minutes. The results are shown in Fig. 5.6.
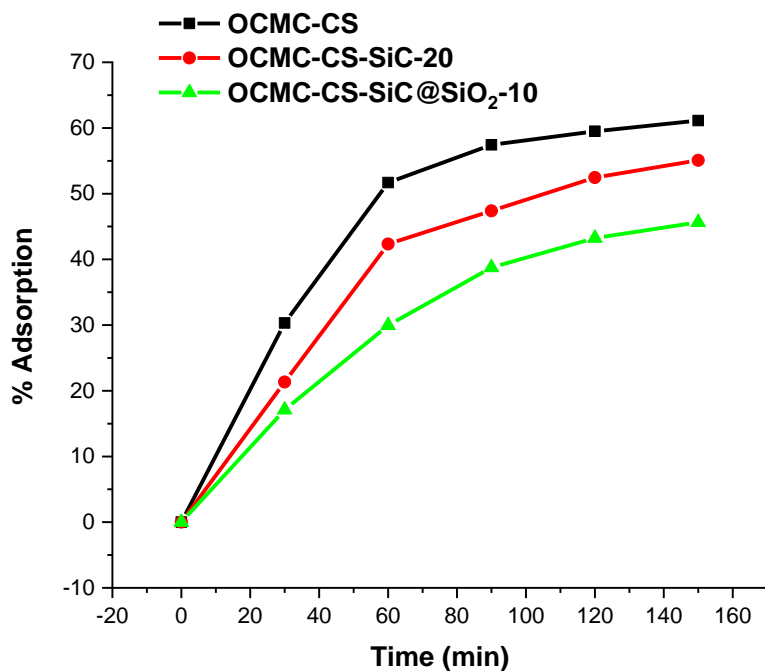

Figure 5.6. Effect of time on the interaction of OCMC-CS, OCMC-CS-SiC-20, and OCMC-CS-SiC@SiO$_2$-10 with MB dye adsorption

Experimental Condition: 100mg of each catalyst was treated against 30 mL of 0.05 mM dye solution for 150 minutes and took reading of absorbance by UV-Vis spectrophotometer for every 30 minutes, at room temperature and at pH 7.

Contact Time	OCMC-CS	OCMC-CS-SiC-20	OCMC-CS-SiC@SiO$_2$-10
0	0	0	0
30	30.32105	21.33621	20.33621
60	47.69441	42.34542	40.34542
90	52.43906	47.3915	45.3915
120	55.49851	50.4673	48.4673
150	56.92403	51.975802	50.0758

Table 5.5. % Adsorption of OCMC-CS, OCMC-CS-SiC-20, and OCMC-CS-SiC@SiO$_2$-10 at 0,30,60,90,120 and 150 minutes.

Adsorption Kinetics

Pseudo-first order (Equation (5.6)) and pseudo-second order (Equation (5.7)) kinetic parameters were calculated.

$$q_t = q_e[1 - \exp(-k_1 t)] \tag{5.6}$$

$$q_t = \frac{q_e^2 k_2 t}{1 + k_2 q_e t} \tag{5.7}$$

where qt (mg/g) represents the quantity of dye adsorbed at time t (min) and qe(mg/g) represents the amount of dye adsorbed at equilibrium. Pseudo-first order and Pseudo-second order constants are denoted by k1 (min^{-1}) and k2 (min^{-1}).

According to Fig. 5.7, 5.8, and the regression coefficient values in Table 2, it is suggested that MB dye adsorption on the OCMC-CS could be successfully explained by a pseudo-1st order, indicating the presence of physisorption and MB dye adsorption on the OCMC-CS-SiC-20 and OCMC-CS-SiC@SiO_2-10 follows the pseudo 2nd order, indicating the presence of chemisorption.
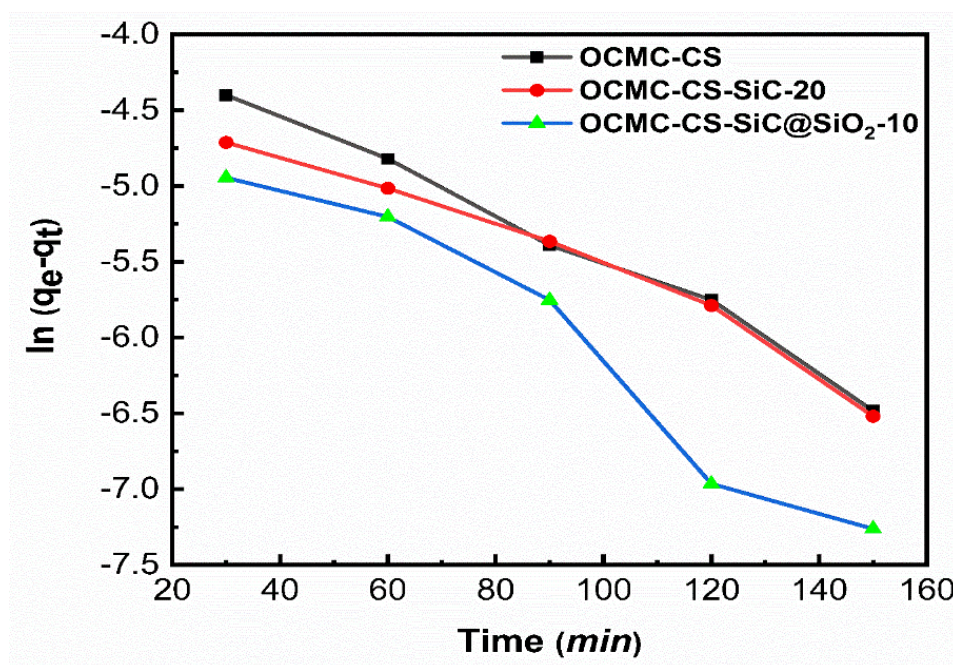

Figure 5.7 Pseudo-first order of OCMC-CS, OCMC-CS-SiC-20, OCMC-CS-SiC@SiO$_2$-10
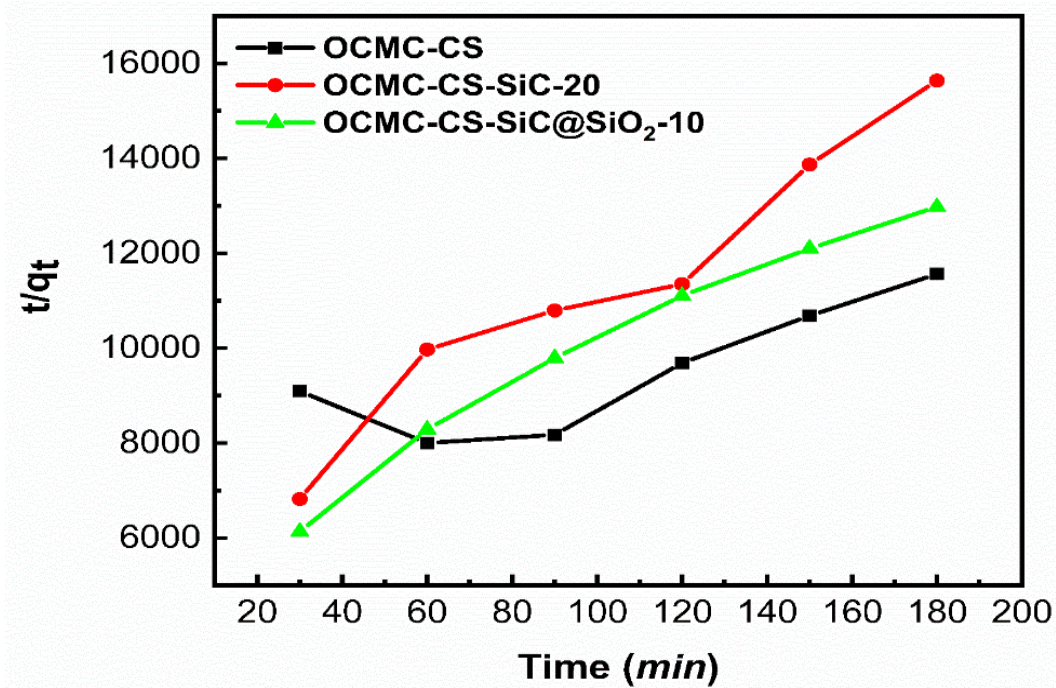
Figure 5.8. Pseudo-second order of OCMC-CS, OCMC-CS-SiC-20, OCMC-CS-SiC@SiO$_2$-10

Catalyst Name	Pseudo 1st order		Pseudo 2nd order	
	K_1	R^2	K_2	R^2
OCMC-CS	1.13×10^{-4}	0.98486	3.12531×10^{-7}	0.62034
OCMC-CS-SiC-20	9.74×10^{-5}	0.9536	9.31117×10^{-8}	0.96609
OCMC-CS-SiC@SiO$_2$-10	1.4×10^{-4}	0.92632	6.01582×10^{-8}	0.94484

Table 5.6 Kinetic parameters for the pseudo-first order, pseudo-second order of OCMC-CS, OCMC-CS-SiC-20, OCMC-CS-SiC@SiO$_2$-10

5.4.3. Effect of Catalyst Dosages

Different amounts of adsorbents (50,100,150 mg) were used to adsorption 30ml of 0.05mM solution of MB dye at room temperature for 150 min at pH 7 (Fig. 5.9). 150mg amount of each adsorbent gave maximum adsorption with MB dye. Adsorption depends on available active sites of adsorbent. With the increase in amount of catalyst, available active sites of adsorbent increased and also the adsorption. With each adsorbent dosage, OCMC-CS gave greater adsorption as compared to the other two catalysts that contain nanoparticles. The reason that the nanoparticles of Si may be blocked the active sites of adsorbents and in this way decreased the adsorption rate.
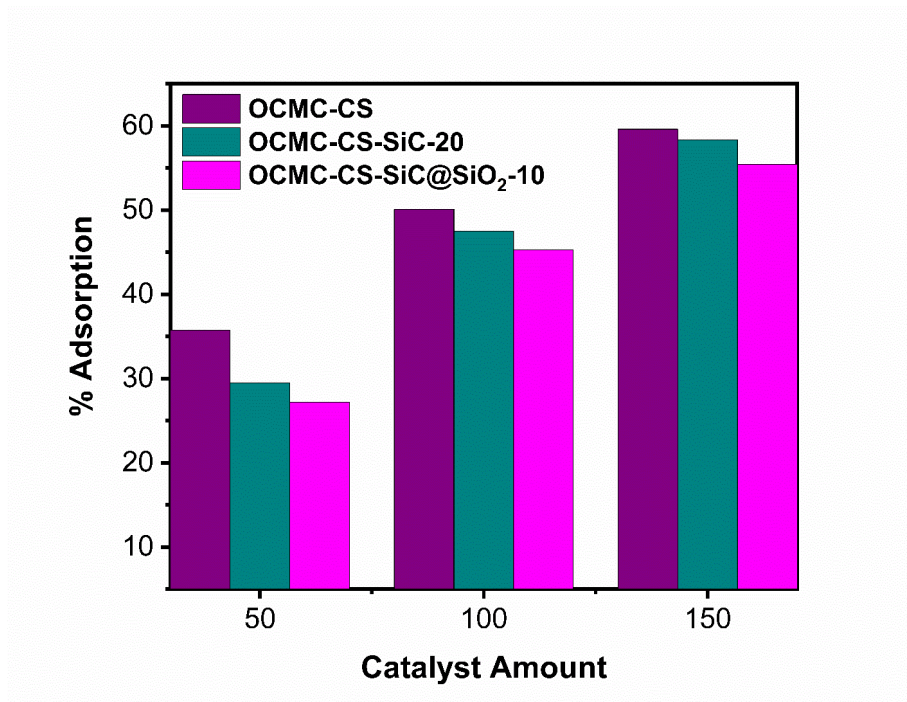

Figure 5.9 Effect of Amount of the catalyst on the interaction of OCMC-CS, OCMC-CS-SiC-20, and OCMC-CS-SiC@SiO$_2$-10 with MB dye adsorption.

Experimental Condition: 50mg, 100mg, 150mg of each catalyst was treated against 30 mL of 0.05 mM dye solution for 150 minutes at room temperature and at pH 7.

Catalyst Amount (mg)	OCMC-CS	OCMC-CS-SiC-20	OCMC-CS-SiC@SiO$_2$-10
50	35.75384	29.4488	27.20121
100	50.0726	47.4934	45.24795
150	59.58116	58.33036	55.40706

Table 5.7 Table: % Adsorption of 50mg, 100mg, 150mg of OCMC-CS, OCMC-CS-SiC-20, and OCMC-CS-SiC@SiO$_2$-10

5.4.4. Effect of pH

The pH of the adsorbent is an important element in the adsorption process because it changes its surface charge. [3]. The effect of pH on the adsorption capacity of OCMC-CS, OCMC-CS-SiC-20, and OCMC-CS-SiC@SiO2-10 samples was studied for 150 minutes using 100 mg of adsorbent and 30ml of 0.05mM MB solution. All studies were conducted at room temperature (25 degrees Celsius). The dye solutions' pH was maintained using 0.1 M HCl and 0.1 M NH4OH solutions. The amount of MB adsorbed was highly dependent on the solution's initial pH (Fig 5.10). The amount of MB adsorption increased as pH increased. The OH- ions in the solution and the functional groups that are present on their surfaces develop a negative charge in a basic media. As a result of competition for adsorption sites between the OH- ions and the MB molecules, cationic MB dye adsorption is most efficient.
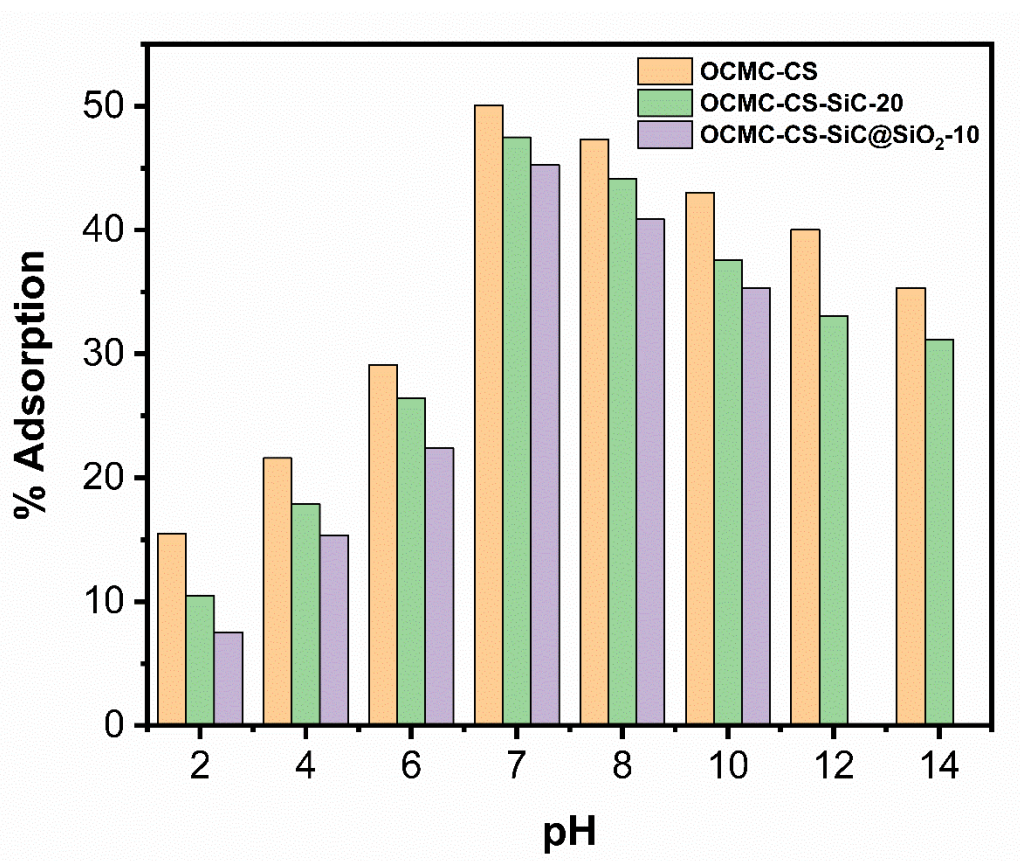
Figure 5.10 Effect of pH of MB dye on the interaction of OCMC-CS, OCMC-CS-SiC-20, and

OCMC-CS-SiC@SiO$_2$-10.

Experimental Condition: 100mg of each catalyst was treated against 30 mL of 0.05 mM dye solution for 150 minutes at room temperature and at different pH.

pH	OCMC-CS	OCMC-CS-SiC-20	OCMC-CS-SiC@SiO$_2$-10
2	15.48218	10.45073	7.71153
4	21.58569	17.85264	15.38227
6	29.11514	26.44923	22.38227
7	50.0726	47.4934	45.24795
8	47.32842	44.15908	40.85504
10	43.03145	37.58491	35.28758
12	40.03412	33.04808	-
14	35.32145	31.16592	-

Table 5.8. % Adsorption of OCMC-CS, OCMC-CS-SiC-20, and OCMC-CS-SiC@SiO$_2$-10 at 2,4,6,7,8,10,12, 14 pH.

Point of Zero Charge

The pH at which the adsorbent's surface exhibits net neutral charge is known as the point of zero charge (pzc). The characterization of the adsorbent is done using pHpzc. According to the results, the pHzpc values for OCMC-CS, OCMC-CS-SiC-20, OCMC-CS-SiC@SiO$_2$-20 were determined to be 5, 5.5 and 6.3, respectively. At pH > pHzpc and pH< pHzpc, the adsorbent has negative and positive surface charges, respectively. Therefore, the surface of the adsorbent will have a net positive charge on which anions may adsorb for a solution whose pH value is lower than the pzc. In contrast, at solution pH levels higher than the pzc, the surface will have a negative charge and

cations will be adsorbed on it. The adsorbent surface needs to be negatively charged in order to adsorb MB dye, which is positively charged. So, pH > pHzpc is necessary for my adsorbents to adsorb cationic MB dye. As shown in Fig 5.11, the pH of OCMC-CS, OCMC-CS-SiC-20, OCMC-CS-SiC@SiO$_2$-20 at point zero charge was established by graphing the graph between pHi and ΔpH. Table 5.9, and 5.10 and Fig. 5.11 display the findings.
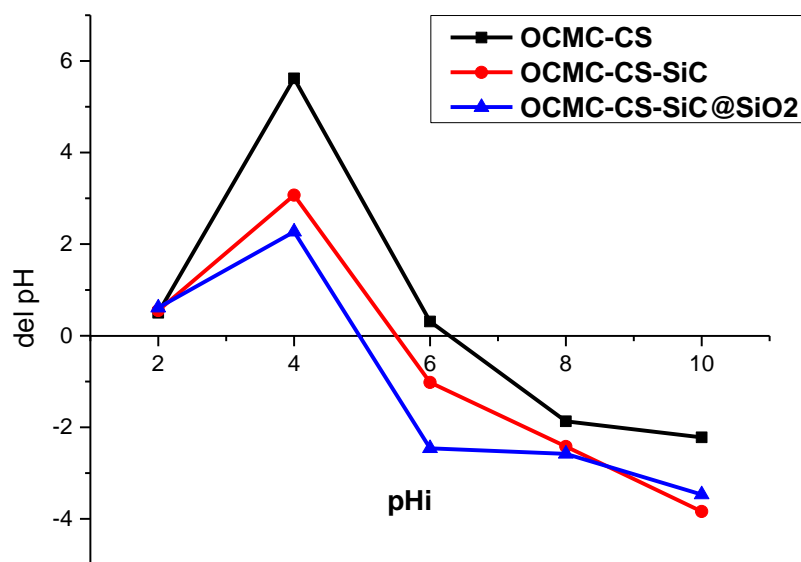

Figure 5.11 Point of zero charge for OCMC-CS, OCMC-CS-SiC-20, OCMC-CS-SiC@SiO$_2$-20

No.	OCMC-CS			OCMC-CS-SiC-20			OCMC-CS-SiC@SiO$_2$-10		
	pHi	pHf	ΔpH	pHi	pHf	ΔpH	pHi	pHf	ΔpH
1	2	2.5	0.5	2	2.55	0.55	2	2.61	0.61
2	4	9.62	5.62	4	7.07	3.07	4	6.27	2.27
3	6	6.31	0.31	6	4.98	-1.02	6	3.54	-2.46
4	8	6.13	-1.87	8	5.58	-2.42	8	5.42	-2.58
5	10	7.78	-2.22	10	6.16	-3.84	10	6.53	-3.47

Table 5.9 pH for point zero charge of OCMC-CS, OCMC-CS-SiC-20, OCMC-CS-SiC@SiO$_2$-20

Adsorbent Name	pH$_{pzc}$
OCMC-CS	5
OCMC-CS-SiC-20	5.5
OCMC-CS-SiC@SiO$_2$-20	6.3

Table 5.10 pH of point zero charge of OCMC-CS, OCMC-CS-SiC-20, OCMC-CS-SiC@SiO$_2$-20

5.4.5. Effect of Temperature

With 30ml 0f 0.05mM solution of MB dye, 100mg of adsorbent, and pH 7 for 150 minutes, the temperature analysis was conducted in the range of 10-70°C. The findings are presented in (Fig. 5.12 and Table 5.11). The findings suggested that the adsorption of OCMC-CS, OCMC-CS-SiC-20, and OCMC-CS-SiC@SiO_2-10 is an endothermic process because the amounts adsorbed increased with rising temperature. This increase results from the greater mobility of MB ions to the adsorbent's surface.
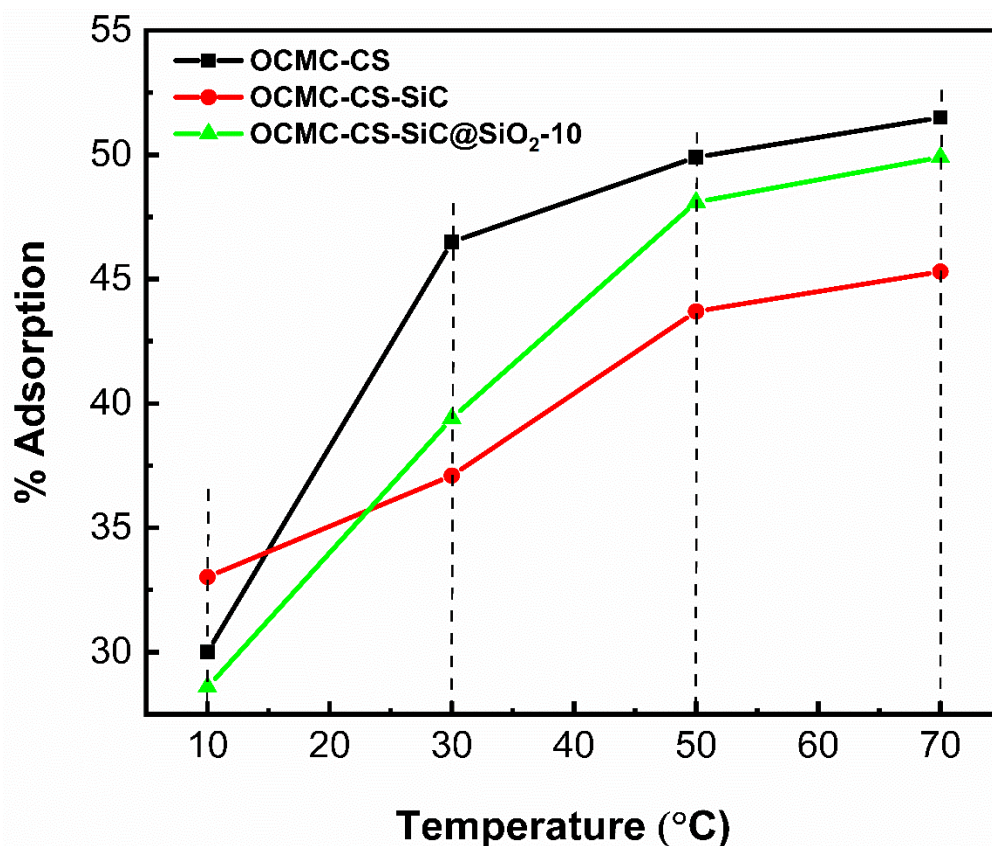
Figure 5.12 Effect of temperature of MB dye on the interaction of OCMC-CS, OCMC-CS-SiC-

20, and OCMC-CS-SiC@SiO_2-10

Experimental Condition: 100mg of each catalyst was treated against 30 mL of 0.05 mM dye solution for 150 minutes at pH 7 at different temperatures.

Temperature	OCMC-CS	OCMC-CS-SiC-20	OCMC-CS-SiC@SiO$_2$-10
10°C	30	33.02	28.6
30°C	46.5	37.1	39.4
50°C	49.5	43.7	48.1
70°C	51.5	45.3	49.9

Table 5.11. % Adsorption of OCMC-CS, OCMC-CS-SiC-20, and OCMC-CS-SiC@SiO$_2$-10 at 10°C, 30°C, 50°C, 70°C

Conclusion

This research successfully developed and characterized oxidized carboxymethyl cellulose-chitosan composite films containing SiC and silica-coated SiC nanoparticles for efficient dye adsorption from aqueous solutions. The study highlights the potential of OCMC-CS films as sustainable adsorbents for the remediation of dye-contaminated wastewater with 55% adsorption efficiency. Further optimization and scale-up studies are recommended to explore their practical applications in real-world scenarios. The findings from this research contribute to the advancement of eco-friendly materials for environmental pollution control and provide a foundation for future research in the field of adsorption science.

References

1. Silva, V.C., et al., *Adsorption behavior of crystal violet and congo red dyes on heat-treated brazilian palygorskite: kinetic, isothermal and thermodynamic studies.* 2021. **14**(19): p. 5688.
2. Omer, O.S., et al., *Adsorption thermodynamics of cationic dyes (methylene blue and crystal violet) to a natural clay mineral from aqueous solution between 293.15 and 323.15 K.* 2018. **11**(5): p. 615-623.
3. Zhu, Z., et al., *Ultrahigh adsorption capacity of anionic dyes with sharp selectivity through the cationic charged hybrid nanofibrous membranes.* 2017. **313**: p. 957-966.
4. Yang, Y., L.J.J.o.Q.S. Wang, and R. Transfer, *Electrically-controlled near-field radiative thermal modulator made of graphene-coated silicon carbide plates.* 2017. **197**: p. 68-75.
5. Rizzi, V., et al., *Applicative study (part I): the excellent conditions to remove in batch direct textile dyes (direct red, direct blue and direct yellow) from aqueous solutions by adsorption processes on low-cost chitosan films under different conditions.* 2014. **4**(04): p. 454.
6. Salama, A. and R.E.J.I.J.o.B.M. Abou-Zeid, *Ionic chitosan/silica nanocomposite as efficient adsorbent for organic dyes.* 2021. **188**: p. 404-410.
7. Ulbricht, M.J.P., *Advanced functional polymer membranes.* 2006. **47**(7): p. 2217-2262.
8. Baker, R.W., K.J.I. Lokhandwala, and E.C. Research, *Natural gas processing with membranes: an overview.* 2008. **47**(7): p. 2109-2121.
9. Fendler, J.H.J.J.o.M.S., *Potential of membrane-mimetic polymers in membrane technology.* 1987. **30**(3): p. 323-346.
10. Loeb, S. and S. Sourirajan, *Sea water demineralization by means of an osmotic membrane*. 1962, ACS Publications.
11. Lee, A., et al., *Membrane materials for water purification: design, development, and application.* 2016. **2**(1): p. 17-42.
12. Egbo, M.K.J.J.o.K.S.U.-E.S., *A fundamental review on composite materials and some of their applications in biomedical engineering.* 2021. **33**(8): p. 557-568.
13. Mansouri, L., et al., *Chemical and biological behaviours of hydrogels based on oxidized carboxymethylcellulose coupled to chitosan.* 2020. **77**(1): p. 85-105.
14. Shariatinia, Z.J.I.j.o.b.m., *Carboxymethyl chitosan: Properties and biomedical applications.* 2018. **120**: p. 1406-1419.
15. Kaur, K. and R.J.C.p. Jindal, *Self-assembled GO incorporated CMC and Chitosan-based nanocomposites in the removal of cationic dyes.* 2019. **225**: p. 115245.
16. Fei Liu, X., et al., *Antibacterial action of chitosan and carboxymethylated chitosan.* 2001. **79**(7): p. 1324-1335.
17. Salehi, E., P. Daraei, and A.A.J.C.p. Shamsabadi, *A review on chitosan-based adsorptive membranes.* 2016. **152**: p. 419-432.
18. Zhao, S.-W., et al., *The preparation and antibacterial activity of cellulose/ZnO composite: A review.* 2018. **16**(1): p. 9-20.
19. An, Z., et al., *Synthesis and formation mechanism of porous silicon carbide stacked by nanoparticles from precipitated silica/glucose composites.* 2019. **54**(4): p. 2787-2795.
20. He, Z.H., et al., *Surface modification of silicon carbide powder with silica coating by rotary chemical vapor deposition.* 2014. **616**: p. 232-236.
21. Kifuani, K.M., et al., *Kinetic and thermodynamic studies adsorption of Methylene Blue (MB) in aqueous solution on a bioadsorbent from Cucumeropsis mannii Naudin waste seeds.* 2018. **12**(5): p. 2412-2423.

22.   Briscoe, B., P. Luckham, and S.J.P. Zhu, *The effects of hydrogen bonding upon the viscosity of aqueous poly (vinyl alcohol) solutions.* 2000. **41**(10): p. 3851-3860.

23.   Sapalidis, A., et al., *Properties of poly (vinyl alcohol)—Bentonite clay nanocomposite films in relation to polymer–clay interactions.* 2012. **123**(3): p. 1812-1821.

24.   Kumar, A., S.S.J.I.j.o.p.m. Han, and p. biomaterials, *PVA-based hydrogels for tissue engineering: A review.* 2017. **66**(4): p. 159-182.

25.   Sapalidis, A.A.J.S., *Porous Polyvinyl alcohol membranes: Preparation methods and applications.* 2020. **12**(6): p. 960.

26.   Teodorescu, M., M. Bercea, and S.J.B.a. Morariu, *Biomaterials of PVA and PVP in medical and pharmaceutical applications: Perspectives and challenges.* 2019. **37**(1): p. 109-131.

27.   Radoor, S., et al., *Adsorption of methylene blue dye from aqueous solution by a novel PVA/CMC/halloysite nanoclay bio composite: Characterization, kinetics, isotherm and antibacterial properties.* 2020. **18**: p. 1311-1327.

28.   Tanzifi, M., et al., *Carboxymethyl cellulose improved adsorption capacity of polypyrrole/CMC composite nanoparticles for removal of reactive dyes: Experimental optimization and DFT calculation.* 2020. **255**: p. 127052.

29.   Abou Taleb, M.F., H. Abd El-Mohdy, and H.J.J.o.h.m. Abd El-Rehim, *Radiation preparation of PVA/CMC copolymers and their application in removal of dyes.* 2009. **168**(1): p. 68-75.

30.   He, X., et al., *Fluorescent hydrogels based on oxidized carboxymethyl cellulose with excellent adsorption and sensing abilities for Ag+.* 2022. **213**: p. 955-966.

31.   López-Valdivieso, A., et al., *Carboxymethylcellulose (CMC) as PbS depressant in the processing of Pb-Cu bulk concentrates. Adsorption and floatability studies.* 2017. **112**: p. 77-83.

32.   Jin, H.-X., et al., *Fabrication of carboxymethylcellulose/metal-organic framework beads for removal of Pb (II) from aqueous solution.* 2019. **12**(6): p. 942.

33.   Ding, W., et al., *Peroxide-periodate co-modification of carboxymethylcellulose to prepare polysaccharide-based tanning agent with high solid content.* 2019. **224**: p. 115169.

34.   Dou, Y., et al., *Preparation and characterization of edible dialdehyde carboxymethyl cellulose crosslinked feather keratin films for food packaging.* 2020. **12**(1): p. 158.

35.   Kulikowska, A., I. Wasiak, and T.J.C.o.M.T. Ciach, *Carboxymethyl cellulose oxidation to form aldehyde group.* 2013. **4**(2).

36.   Li, H., et al., *Concomitant degradation in periodate oxidation of carboxymethyl cellulose.* 2011. **84**(3): p. 881-886.

37.   Ogushi, Y., et al., *Synthesis of enzymatically-gellable carboxymethylcellulose for biomedical applications.* 2007. **104**(1): p. 30-33.

38.   Sharma, A.K., et al., *Borax mediated synthesis of a biocompatible self-healing hydrogel using dialdehyde carboxymethyl cellulose-dextrin and gelatin.* 2021. **166**: p. 104977.

39.   Shen, Y., et al., *pH and redox dual stimuli-responsive injectable hydrogels based on carboxymethyl cellulose derivatives.* 2016. **24**: p. 602-608.

40.   Hivechi, A., et al., *Oxidized carboxymethyl cellulose/gelatin in situ gelling hydrogel for accelerated diabetic wound healing: Synthesis, characterization, and in vivo investigations.* 2023: p. 125127.

41.   Yu, X., et al., *'Multiple and short-range'cross-linking of dialdehyde carboxymethyl cellulose contributes to regulating the physicochemical property of collagen fibril.* 2022. **219**: p. 21-30.

42.   Mao, X., et al., *Synthesis of a three-dimensional network sodium alginate–poly (acrylic acid)/attapulgite hydrogel with good mechanic property and reusability for efficient adsorption of Cu 2+ and Pb 2+.* 2018. **16**: p. 653-658.

43.   Mekuria, T.D., C. Zhang, and D.E.J.C.P.B.E. Fouad, *The effect of thermally developed SiC@ SiO2 core-shell structured nanoparticles on the mechanical, thermal and UV-shielding properties of polyimide composites.* 2019. **173**: p. 106917.

44.   Fifield, F.W., *Principles and practice of analytical chemistry*. 2000.

45.   Benghanem, S., et al., *Grafting of oxidized carboxymethyl cellulose with hydrogen peroxide in presence of Cu (II) to chitosan and biological elucidation.* 2017. **37**(1): p. 94-102.

46.   Olad, A., et al., *Synthesis, characterization, and swelling kinetic study of porous superabsorbent hydrogel nanocomposite based on sulfonated carboxymethylcellulose and silica nanoparticles.* 2018. **25**: p. 1325-1335.